Trajectory PHD and CPHD Filters With Unknown Detection Profile

Shaoxiu Wei, Boxiang Zhang, and Wei Yi, *Senior Member, IEEE*

***Abstract*—Compared to the probability hypothesis density (PHD) and cardinalized PHD (CPHD) filters, the trajectory PHD (TPHD) and trajectory CPHD (TCPHD) filters are for sets of trajectories, and thus are able to produce trajectory estimates with better performance. In this paper, we develop the TPHD and TCPHD filters which can adaptively learn the history of the unknown target detection probability, and therefore they can perform more robustly in scenarios where targets are with unknown and time-varying detection probabilities. These filters are referred to as the unknown TPHD (U-TPHD) and unknown TCPHD (U-TCPHD) filters. By minimizing the Kullback-Leibler divergence (KLD), the U-TPHD and U-TCPHD filters can obtain, respectively, the best Poisson and independent identically distributed (IID) density approximations over a set of augmented trajectories. For computational efficiency, we also propose the U-TPHD and U-TCPHD filters that only consider the unknown detection profile at the current time. Specifically, the Beta-Gaussian mixture method is adopted for the implementations of proposed filters, which are referred to as the BG-U-TPHD and BG-U-TCPHD filters. The L-scan approximations of these filters with much lower computational burden are also presented. Finally, various simulation results demonstrate that the BG-U-TPHD and BG-U-TCPHD filters can achieve robust tracking performance to adapt to unknown detection profile. Besides, it also shows that usually a small value of L in the L-scan approximation has similar performance than with a large value at a fraction of the computational cost.**

***Index Terms*—Beta-Gaussian mixture, sets of trajectories, trajectory PHD filter, trajectory CPHD filter, unknown detection probability.**

I. Introduction

The purpose of multi-target tracking is to estimate the time-varying number and states of targets through a set of measurements in the presence of data association uncertainty, detection uncertainty, false measurements, and noise [1]–[6]. There are three main approaches to multi-target tracking: the joint probabilistic data association (JPDA) filter [7], [8], the multiple hypotheses tracking (MHT) [1], [9] and the random finite set (RFS) [10]. Among them, the RFS approaches aim to model the appearance and disappearance of targets, misdetections and false alarms within a unified Bayesian framework [10].

Several tractable and useful multi-object filters have been developed based on RFS methods, including the probability hypothesis density (PHD) filter [10]–[12], the cardinalized PHD (CPHD) filter [10], [13], [14], the multi-Bernoulli (MB) filter [10], [15], the Poisson multi-Bernoulli mixture (PMBM) filter [16], [17], the generalized labeled multi-Bernoulli (GLMB) filter [18], [19], and the labeled multi-Bernoulli (LMB) filter [20]. Among them, the PHD and CPHD filters are the most fundamental RFS filters and known for their low computational burden. The PHD filter considers a Poisson multi-target filtering density, while the CPHD filter considers an independent and identically distributed (IID) cluster multi-target filtering density. If the prior or posterior density is not Poisson or IID cluster, the PHD and CPHD filters can be achieved using the best Poisson or IID cluster approximations that minimizes the Kullback-Leibler divergence (KLD) [21]. When we do not consider the target spawning, the Poisson prior in the PHD filter can be directly achieved by the Poisson posterior at the last time step and Poisson birth at the current time step. Both filters can be implemented efficiently using numerical solutions such as sequential Monte Carlo (SMC) [22], [23], or Gaussian mixture (GM) [12], [14]. In recent years, the PHD and CPHD filters have also been successfully applied to the distributed multi-sensor fusion [24], [25], robotics [26], [27] and visual tracking [28], [29].

All the aforementioned filters use a set of targets as the state variable, and update the filtering density at each measurement time. Because the filtering density only captures the statistical information on the current multi-target state variable, the historical estimates cannot be updated with the subsequent measurements. As a result, these filtering density based filters usually have poorer performance compared to the smoothing methods [30]. Besides, without the assistance of the target labels (or tags), the unlabeled filters such as the PHD and CPHD filters can not form target trajectories.

Recently, the trajectory PHD (TPHD) and trajectory cardinalized PHD (TCPHD) filters are proposed by adopting a set of trajectories as the state variable [31], [32]. In this way, the TPHD and TCPHD filters are able to establish trajectories directly and output better estimation performance than the standard PHD and CPHD filters. Specifically, based on the KLD minimization, the TPHD and TCPHD filters propagate the best approximated PHD of the Poisson and IID cluster multi-trajectory densities respectively. The TPHD and TCPHD filters do not marginalize

Manuscript received 15 April 2021; revised 12 August 2021, 22 November 2021, 24 March 2022, and 20 April 2022; accepted 4 May 2022. Date of publication 10 May 2022; date of current version 15 August 2022. This work was supported in part by the National Natural Science Foundation of China under Grants 61771110, U19B2017 and 61871103, in part by the Fundamental Research Funds of Central Universities under Grant ZYGX2020ZB029, in part by Chang Jiang Scholars Program, and in part by the 111 Project under Grant B17008. The review of this article was coordinated by Prof. Mugen Peng. *(Corresponding author: Wei Yi.)*

The authors are with the School of Information and Communication Engineering, University of Electronic Science and Technology of China, Chengdu, Sichuan 611731, China (e-mail: sxiu_wei@qq.com; 201811011921@std.uestc.edu.cn; kussoyi@gmail.com).

Digital Object Identifier 10.1109/TVT.2022.3174055

the past target states in the prediction step and are able to update the PHD of whole trajectory using current measurements. This is also why the TPHD and TCPHD filters can outperform the standard PHD and CPHD filters. In [32], the Gaussian mixture (GM) implementations for the TPHD and TCPHD filters are also proposed and referred to as GM-TPHD and GM-TCPHD. Meanwhile, the L-scan approximation strategy is suggested to achieve the fast implementation by only updating the multi-trajectory density of the last L time. Following the same routine, the trajectory MB (TMB) filter and the trajectory PMBM (TPMBM) filter have also been devised recently [33], [34]. In [30], by adopting a set of trajectories as the state variable, a multi-scan version of the GLMB filter is proposed to directly propagate the labeled multi-trajectory posterior density. The multi-scan GLMB recursion does not marginalize over the past label sets and the past trajectory states, and in principle the multi-trajectory posterior contains the complete statistical characterization of the interested variables based on all the historical measurement sets. Consequently, the multi-scan GLMB filter can provide excellent estimation performance of target trajectories. On the other hand, techniques such as component truncation and Gibbs sampler need to be employed to enable an efficient implementation [18], [19], [30].

In multi-target tracking, the knowledge of two uncertain sources, namely, the clutter rate and detection probability are also of significant importance. However, in many practical applications, the clutter rate and detection probability change dynamically between time steps in unpredictable ways. In general, it is difficult to infer these characteristics from training data. Rather they should be inferred online from the actual measurement sequence [35]. To deal with issues of unknown clutter rate, the robust PHD/CPHD filters based on a clutter generator have been proposed [35]–[38]. These methods assume that the multi-target state consists of both the finite sets of actual targets and clutter generators, and can obtain clutter information by tracking those clutter generators [38]. As for the unknown detection probability, several improved filters have been proposed to adaptively estimate the unknown detection profile [38]–[43]. For example, the augmented state model is proposed to adopt the unknown detection profile using the Beta-Gaussian mixtures in the PHD and CPHD filters [38]. Later, the inverse Gamma-Gaussian mixture is employed to propagate non-negative features, including signal amplitude and SNR, which are non-Gaussian [43].

In this paper, we aim to develop the TPHD and TCPHD filters which can perform robustly in scenarios with unknown and time-varying target detection probability, and they are referred to as the unknown TPHD (U-TPHD) and unknown TCPHD (U-TCPHD) filters. Specifically, during the derivations of U-TPHD and U-TCPHD, the Beta-Gaussian mixture approach [38] is chosen to obtain a closed form solution, where the Beta distribution is used to model the detection probability. The main contributions are given as follows:

1) *Derivations of recursive equations for the U-TPHD/U-TCPHD filters:* Generally, the TPHD and TCPHD filters propagate forward the PHD of Poisson and IID cluster multi-trajectory densities, respectively. In principle, by augmenting the sequence of the unknown detection probabilities into a set of trajectories, the proposed filters can not only adaptively learn the uneven detection profile, but also obtain the information about target trajectories. Similarly, the KLD minimization is adopted to avoid the non-Poisson posterior in the U-TPHD filter and non-IID prior and posterior in the U-TCPHD filter. Besides, considering computation efficiency, the analytic recursions are also presented for the U-TPHD and U-TCPHD filters, which only consider the effect of the unknown detection probability at the latest frame time.
2) *The Beta-Gaussian mixture implementations for the U-TPHD and U-TCPHD filters:* In the algorithmic implementation, the set of augmented trajectories is modeled by using the Beta-Gaussian (BG) mixtures, where each component is the product of a Beta density (on the augmented part) and a Gaussian density (on the trajectory) [38]. The resulting filters are named as the BG-U-TPHD and BG-U-TCPHD filters for short. In consideration of the algorithmic complexity, we also propose the approximated versions of the BG-U-TPHD and BG-U-TCPHD filters, which only consider the unknown detection profile at the current time. The L-scan approximations of these filters are also proposed to achieve lower computational costs.

The remainder of the paper is organized as follows. Section II presents the background materials on the TPHD and TCPHD filters. In Section III, the detail derivations of the proposed U-TPHD and U-TCPHD filters are given. Their Beta-Gaussian mixture implementations and the corresponding L-scan approximations are developed in Section IV. The estimation step including pruning and absorption procedures is also delineated in this section. The performance assessments of the proposed filters are given in Section V. Lastly, conclusions are given in Section VI.

II. Background

This section provides a brief review of the trajectory RFS, the TPHD and TCPHD filters. Notations are first given in Section II-A. In Section II-B, the Bayesian recursions for the TPHD and TCPHD filters are reviewed. The prediction and update steps of the TPHD and TCPHD filters are provided in Section II-C. Further details are available in [32].

A. Notations

The variable $X = (t, x^{1:i})$ with $x \in \mathbb{R}^{n_x}$ is used to denote a single trajectory, where t represents its birth time, n_x is the dimension of target state x and $x^{1:i} = (x^1, \ldots, x^i)$ denotes a sequence of target states with length i. At time k, the trajectory state space is defined as

$$\mathbb{T}_k = \uplus_{(t,i)\in\mathbb{I}_k} \{t\} \times \mathbb{R}^{in_x}, \tag{1}$$

where $\uplus$ denotes the disjoint union, $\times$ denotes a Cartesian product, and $\mathbb{I}_k$ is a discrete variable state space that equals to $\{(t, i) : 1 \leq t \leq k \text{ and } 1 \leq i \leq k - t + 1\}$. A single trajectory density is given as $\bar{p}(X)$ and its integral is expressed as [44]

$$\int_{\mathbb{T}} \bar{p}(X)dX = \sum_{(t,i)\in\mathbb{I}} \int_{\mathbb{R}^{in_x}} \bar{p}\left(t, x^{1:i}\right) dx^{1:i}. \tag{2}$$

Similar to the target RFS, the trajectory RFS at time k is defined as

$$\mathbf{X}_k = \{X_1, \ldots, X_{N^k}\} \in \mathcal{F}(\mathbb{T}_k), \tag{3}$$

where $\mathcal{F}(\mathbb{T}_k)$ is the respective collections of all finite subsets of $\mathbb{T}_k$ defined by (1). The PHD of posterior multi-trajectory density at time k is denoted as $D_k(X)$. Given a trajectory X, the corresponding target state at time k is given as $\tau_k(X)$. Similarly, given the multi-trajectory state $\mathbf{X}_k$, the multi-target state is $\tau_k(\mathbf{X}_k) = \cup_{X\in\mathbf{X}_k}\tau_k(X)$.

The single trajectory state is denoted by using the uppercase letter (e.g. X), whose subscript represents the number (e.g. X_j). The multi-trajectory state is represented by the bold letter (e.g. $\mathbf{X}$), whose subscript only represents the time (e.g. $\mathbf{X}_k$). The binomial coefficient and the permutation coefficient notations are given as, respectively, $C_j^\ell = \frac{\ell!}{j!(\ell-j)!}$ and $P_j^\ell = \frac{\ell!}{(\ell-j)!}$. For discrete variables A and B, the generalized Kronecker delta function is given as

$$\delta_A[B] \triangleq \begin{cases} 1, & \text{if } A = B \\ 0, & \text{otherwise.} \end{cases} \tag{4}$$

If both A and B are continuous variables, we use $\delta_A(B)$ instead. Besides, the inner product between two real valued functions a and b is expressed as $\langle a, b\rangle$, which also equals to $\int a(x)b(x)dx$. If a and b are both real sequences, their inner product is written as $\langle a, b\rangle = \sum_{n=0}^{\infty} a(n)b(n)$. For a finite set $\mathcal{Z}$ of real numbers, its *elementary symmetric function* [45] of order q is given as

$$e_q\left(\mathcal{Z}\right) = \sum_{\sigma\subseteq\mathcal{Z},|\sigma|=q} \prod_{\xi\in\sigma} \xi, \tag{5}$$

and the subtraction of sets is represented by the notation $\backslash$.

B. Bayesian Filtering Recursion

The multi-trajectory state and set of measurements at time k are the finite sets expressed as follows,

$$\mathbf{X}_k = \{X_1, \ldots, X_{N^k}\} \in \mathcal{F}(\mathbb{T}_k), \tag{6}$$

$$Z_k = \{z_1, \ldots, z_{M^k}\} \in \mathcal{F}(\mathbb{Z}_k). \tag{7}$$

where N^k trajectories take values in the state space $\mathbb{T}_k$ and M^k measurements take values in the measurement space $\mathbb{Z}_k \triangleq \mathbb{R}^{n_z}$.

If the posterior multi-trajectory density p_{k-1} at time $k-1$ is given, the posterior density at time k can be computed by using the Bayesian recursion [32]

$$p_{k|k-1}\left(\mathbf{X}_k\right) = \int f\left(\mathbf{X}_k|\mathbf{X}_{k-1}\right) p_{k-1}\left(\mathbf{X}_{k-1}\right)\delta\mathbf{X}_{k-1}, \tag{8}$$

$$p_k\left(\mathbf{X}_k\right) = \frac{\ell_k\left(Z_k|\mathbf{X}_k\right) p_{k|k-1}\left(\mathbf{X}_k\right)}{\int \ell_k\left(Z_k|\mathbf{X}_k\right) p_{k|k-1}\left(\mathbf{X}_k\right)\delta\mathbf{X}_k}, \tag{9}$$

where $f(\mathbf{X}_k|\mathbf{X}_{k-1})$ denotes the transition density of trajectories and $p_{k|k-1}(\mathbf{X}_k)$ denotes the predicted multi-trajectory density at time k. Given a set of trajectories $\mathbf{X}_k$, the density of measurements Z_k is denoted as $\ell_k(Z_k|\mathbf{X}_k)$. Since the current measurements are only based on potential target states at the current time, $\ell_k(Z_k|\mathbf{X}_k)$ can be also written as

$$\ell_k\left(Z_k|\mathbf{X}_k\right) = \ell_k\left(Z_k|\tau_k\left(\mathbf{X}_k\right)\right). \tag{10}$$

Thus, for a single trajectory $\underline{X} = (\underline{t}, \underline{x}^{1:\underline{i}})$ at time $k-1$, its measurement likelihood function is expressed as $l_{k-1}(z|\underline{x}^{\underline{i}})$ and its transition density to the trajectory state $X = (t, x^{1:i})$ at time k is expressed as:

$$f\left(X|\underline{X}\right) = f\left(x^i|x^{i-1}\right)\delta_{\underline{x}^{1:\underline{i}}}(x^{1:i-1})\delta_{\underline{t}}[t]\delta_{\underline{i}+1}[i]. \tag{11}$$

C. The TPHD and TCPHD Filters

1) Poisson Trajectory RFS: The TPHD filter propagates the Poisson multi-trajectory density [32], with a KLD minimization after the update step. At time k, the posterior multi-trajectory density $p(\cdot)$ of a Poisson RFS is given as

$$p_k(\{X_1, \ldots, X_{N^k}\}) = e^{-\lambda_k}\lambda_k^n \prod_{j=1}^{N^k} \bar{p}_k(X_j), \tag{12}$$

where $\bar{p}_k(\cdot)$ represents a single trajectory density and $\lambda_k \geq 0$. A Poisson PDF can be characterized by its intensity $D_k(X) = \lambda_k\bar{p}_k(X)$ [32]. Meanwhile, the clutter RFS is Poisson with mean λ_c and density $\bar{c}(\cdot)$.

Based on the following assumptions:

- The trajectories at the current time are the union of the current new trajectories and the surviving trajectories at the last time. The new born trajectories are Poisson with the PHD $\gamma(\cdot)$. The survival probability is given as $p_S(\cdot)$. Note that, the birth and survival RFSs are independent of each other.
- The trajectory RFS at time $k-1$ is Poisson. The clutter is also Poisson and independent of target-originated measurements.

If at time $k-1$, the posterior PHD $D_{k-1}(t, x^{1:i-1})$ is given, the prediction step of the TPHD filter for $X = (t, x^{1:i})$ is expressed as

$$D_{k|k-1}(X) = \gamma_k(X) + D_k^{\zeta}(X), \tag{13}$$

where

$$\gamma_k\left(t, x^{1:i}\right) = \gamma\left(t, x^{1:i}\right)\delta_1[i]\delta_k[t], \tag{14}$$

$$D_k^{\zeta}\left(t, x^{1:i}\right) = p_{S,k}\left(x^{i-1}\right) f\left(x^i|x^{i-1}\right) D_{k-1}\left(t, x^{1:i-1}\right). \tag{15}$$

Please note that, the value of t in (15) belongs to the set $\{1, 2, \ldots, k-1\}$. The TPHD filter only predicts the PHD of alive trajectories [32], and thus the predicted PHD D_k^{ζ} is zero if $t + i - 1 \neq k$. The notation $f(\cdot|\cdot)$ represents the transition density of target in (15). The update step of the TPHD filter is given by

$$\begin{aligned} D_k(X) &= D_{k|k-1}(X)q_{D,k}\left(x^i\right) \\ &\quad + D_{k|k-1}(X)p_{D,k}(x^i) \\ &\quad \times \sum_{z\in Z_k} \frac{l_k(z|x^i)}{\lambda_c \bar{c}(z) + \left\langle p_{D,k}\cdot l_k\left(z|\cdot\right), D^{\tau}_{k|k-1}\right\rangle}, \end{aligned} \tag{16}$$

where

$$D^{\tau}_{k|k-1}\left(x^i\right) = \sum_{t=1}^{k} \int D_{k|k-1}(t, x^{1:k-t+1}) dx^{1:k-t}, \tag{17}$$

which denotes the PHD of the prior multi-target density at time k and is obtained by the marginalization for the PHD of the Poisson multi-trajectory density [32]. The detection probability is denoted as $p_{D,k}(\cdot)$ and the notation $q_{D,k}$ equals to $1 - p_{D,k}$.

2) IID Cluster Trajectory RFS: The TCPHD filter considers an IID cluster multi-trajectory density [32]. At time k, the posterior multi-trajectory density $p_k(\cdot)$ of an IID cluster RFS is given as

$$p_k(\{X_1, \ldots, X_{N^k}\}) = \rho_k(n)n! \prod_{j=1}^{N^k} \bar{p}_k(X_j), \tag{18}$$

where $\rho_k(\cdot)$ is the cardinality distribution and $\bar{p}_k(\cdot)$ is the single trajectory density. The PHD of posterior multi-trajectory density is given as

$$D_k(X) = \bar{p}_k(X) \sum_{n=0}^{\infty} n\rho_k(n). \tag{19}$$

Based on the following assumptions:

- The trajectories at time k are the union of the surviving trajectories at time $k-1$ and the current new trajectories with cardinality distribution $\rho_{\gamma,k}(\cdot)$. Similarly, the birth and survival RFSs are independent of each other.
- Both the trajectory RFS and the clutter RFS are IID cluster. The cardinality distribution of trajectory and clutter are respectively given as $\rho_k(\cdot)$ and $\rho_{c,k}(\cdot)$. The clutter is independent of target-originated measurements.

Based on the KLD minimization, the TCPHD filter propagates both the PHD of the IID multi-trajectory densities and the cardinality distribution [21]. Given the posterior cardinality distribution $\rho_{k-1}(\cdot)$ and posterior PHD $D_{k-1}(t, x^{1:i-1})$ at time $k-1$, the prediction step of the TCPHD filter for $X = (t, x^{1:i})$ is obtained by

$$D_{k|k-1}(X) = \gamma_k(X) + D^{\zeta}_k(X), \tag{20}$$

$$\begin{aligned} \rho_{k|k-1}(n) &= \sum_{j=0}^{n} \rho_{\gamma,k}\left(n-j\right) \sum_{\ell=j}^{\infty} C^{\ell}_j \rho_{k-1}\left(\ell\right) \\ &\quad \times \frac{\left\langle p_{S,k}, D^{\tau}_{k-1}\right\rangle^j \left\langle 1-p_{S,k}, D^{\tau}_{k-1}\right\rangle^{\ell-j}}{\left\langle 1, D^{\tau}_{k-1}\right\rangle^{\ell}}. \end{aligned} \tag{21}$$

The update step of the TCPHD filter is expressed as

$$\rho_k(n) = \frac{\Upsilon^0_k\left[D^{\tau}_{k|k-1}; z_k\right](n)\rho_{k|k-1}(n)}{\left\langle \Upsilon^0_k\left[D^{\tau}_{k|k-1}; z_k\right], \rho_{k|k-1}\right\rangle}, \tag{22}$$

$$\begin{aligned} D_k(X) &= D_{k|k-1}(X)q_{D,k}\left(x^i\right) \\ &\quad \times \frac{\left\langle \Upsilon^1_k\left[D^{\tau}_{k|k-1}; Z_k\right], \rho_{k|k-1}\right\rangle}{\left\langle \Upsilon^0_k\left[D^{\tau}_{k|k-1}; Z_k\right], \rho_{k|k-1}\right\rangle} \\ &\quad + D_{k|k-1}(X)p_{D,k}\left(x^i\right) \\ &\quad \times \sum_{z\in Z_k} \frac{l_k\left(z|x^i\right)}{\bar{c}(z)} \frac{\left\langle \Upsilon^1_k\left[D^{\tau}_{k|k-1}; Z_k\backslash\{z\}\right], \rho_{k|k-1}\right\rangle}{\left\langle \Upsilon^0_k\left[D^{\tau}_{k|k-1}; Z_k\right], \rho_{k|k-1}\right\rangle}, \end{aligned} \tag{23}$$

where

$$\begin{aligned} &\Upsilon^u\left[D^{\tau}_{k|k-1}, Z_k\right](n) \\ &= \sum_{j=0}^{\min\left(M^k, n-u\right)} \left(M^k - j\right)! \rho_{c,k}\left(M^k - j\right) \\ &\quad \times P^n_{j+u} \frac{\left\langle q_{D,k}, D^{\tau}_{k|k-1}\right\rangle^{n-j-u}}{\left\langle 1, D^{\tau}_{k|k-1}\right\rangle^{n}} e_j\left(\Xi\left(D^{\tau}_{k|k-1}, Z_k\right)\right), \end{aligned} \tag{24}$$

$$\begin{aligned} &\Xi\left(D^{\tau}_{k|k-1}, Z_k\right) \\ &= \left\{\int p_{D,k}\left(x^i\right) \frac{l_k\left(z|x^i\right)}{\bar{c}(z)} D^{\tau}_{k|k-1}\left(x^i\right) dx^i : z\in Z_k\right\}. \end{aligned} \tag{25}$$

The TPHD and TCPHD filters can be effectively implemented by the Gaussian mixtures [32], which are respectively referred to as the GM-TPHD and GM-TCPHD filters. Besides, the pruning and absorption procedures are also proposed to prevent an unbounded increase of Gaussian components.

III. Trajectory PHD and CPHD Filters With Unknown Detection Profile

In this section, the prediction and update steps of the U-TPHD and U-TCPHD filters are elaborated. Both filters propagate the PHD of augmented trajectories, which can not only learn the uneven detection profile, but also obtain trajectory estimates. In principle, by updating the information about sequences of the detection probabilities, both filters can perform more robustly in scenarios where targets are with unknown and time-varying detection probabilities than considering these detection probabilities at a single frame time.

A. The Augmented State Space Model

Let $\mathbb{U}_k$ represent the space of augmented trajectories and $\mathbb{D}^i$ denote the space of the sequence of the unknown detection probabilities, where $\mathbb{D}$ denotes the space in the interval of [0, 1].

Then, the augmented trajectory space model is defined as

$$\mathbb{U}_k = \uplus_{(t,i)\in\mathbb{I}_k}\{t\}\times\mathbb{R}^{i\times n_x}\times\mathbb{D}^i. \tag{26}$$

Supposing that at time k, there are N^k augmented trajectories taking values in the state space $\mathbb{U}_k$, then the augmented trajectory RFS is given as

$$\tilde{\mathbf{X}}_k = \{\tilde{X}_1,\ldots,\tilde{X}_{N^k}\}\in\mathcal{F}(\mathbb{U}_k), \tag{27}$$

which is a simple development of trajectory RFS. Each element of $\tilde{\mathbf{X}}$ denotes an augmented trajectory state and is expressed as

$$\tilde{X} = (X, A)\in\mathbb{U}, \tag{28}$$

which consists of the trajectory state $X=(t,x^{1:i})\in\mathbb{T}$ and the sequence of detection probabilities $A=a^{1:i}\in\mathbb{D}^i$. On the other hand, at each time step of the augmented trajectory, we can obtain the augmented target state $\tilde{x}=(x,a)$, where $a\in\mathbb{D}$ denotes the detection probability and x denotes the target state. The density of a single augmented trajectory is given as $\bar{p}(\tilde{X})$ and its integral is

$$\int_{\mathbb{U}}\bar{p}\left(\tilde{X}\right)d\tilde{X} = \sum_{(t,i)\in\mathbb{I}}\int_{\mathbb{R}^{in_x}}\int_{\mathbb{D}^i}\bar{p}\left(t,x^{1:i},a^{1:i}\right)da^{1:i}dx^{1:i}. \tag{29}$$

The density of a set of augmented trajectories is defined as the augmented multi-trajectory density. In this paper, the detection probability at time k is given as

$$p_{D,k}(\tilde{X}) = a^i, \tag{30}$$

where $i=k-t+1$. The transition density of the augmented trajectory is given as $\tilde{f}(\tilde{X}|\underline{\tilde{X}})$, where $\underline{\tilde{X}}=(\underline{t},\underline{x}^{1:\underline{i}},\underline{a}^{1:\underline{i}})$ denotes the augmented trajectory at time $k-1$. To better explain the relationship between the detection probability sequence and trajectory, we consider the transition of detection probability is independent of the trajectory state and it is the first-order Markov process. Then, the equation is established as follows

$$\begin{aligned}\tilde{f}\left(\tilde{X}|\underline{\tilde{X}}\right) &= \tilde{f}\left(t,x^{1:i},a^{1:i}|\underline{t},\underline{x}^{1:\underline{i}},\underline{a}^{1:\underline{i}}\right)\\ &= f\left(x^i|x^{i-1},a^{i-1}\right)g\left(a^i|a^{i-1}\right)\delta_{\underline{x}^{1:\underline{i}}}(x^{1:i-1})\\ &\quad\times\delta_{\underline{a}^{1:\underline{i}}}(a^{1:i-1})\delta_{\underline{t}}[t]\delta_{\underline{i}+1}[i],\end{aligned} \tag{31}$$

where $f(\cdot|\cdot)$ and $g(\cdot|\cdot)$ represents the transition density of target and detection probability from time $k-1$ to k, respectively.

Given the augmented trajectory $\tilde{X}$, the PHD of the augmented multi-trajectory density at time k is denoted as $D_k(\tilde{X})$ and the survival probability of the augmented trajectory is given as

$$p_{S,k}\left(\tilde{X}\right) = p_{S,k}(X,A) = p_{S,k}\left(x^i\right). \tag{32}$$

The current measurements are based on potential target states at the current time [32], so the measurement likelihood function $l_k(z|\tilde{X})$ for a single measurement z is given as

$$l_k\left(z|\tilde{X}\right) = l_k\left(z|x^i\right). \tag{33}$$

B. The U-TPHD Filter

In this section, the recursion of the U-TPHD filter is derived in detail, which predicts and updates the PHD of trajectories and detection probability sequences rather than that of target states and detection probabilities only at the latest frame time [38]. To solve the problem that updated posterior augmented multi-trajectory density is no longer Poisson, the U-TPHD filter finds the best Poisson approximation through the KLD minimization [21]. Based on this theory, the U-TPHD filter propagates the PHD of the Poisson augmented multi-trajectory density through recursions. The prediction and update steps are given in Propositions 1 and 2, respectively.

The recursion of the U-TPHD filter follows the routine of:

Assumption 1: The trajectories are the superposition of alive trajectories at the last time and new births at the current time, which are independent of each other. The PHD of the born trajectory with the augmented part is given as $\gamma(\tilde{X})$ and the birth model is assumed as known.

Assumption 2: The clutter RFS is Poisson with mean λ_c and density $\bar{c}(\cdot)$. The clutter is independent of target generated measurements.

Assumption 3: Each trajectory generates measurements independently of each other.

Assumption 4: The prior and posterior augmented multi-trajectory densities are Poisson.

Proposition 1: If at time $k-1$, the posterior PHD $D_{k-1}(t,x^{1:i-1},a^{1:i-1})$ is given, then the predicted PHD $D_{k|k-1}(\cdot)$ for $\tilde{X}=(t,x^{1:i},a^{1:i})$ is given as

$$D_{k|k-1}\left(\tilde{X}\right) = \gamma_k\left(\tilde{X}\right) + D_k^{\zeta}\left(\tilde{X}\right), \tag{34}$$

where

$$\gamma_k\left(t,x^{1:i},a^{1:i}\right) = \gamma\left(t,x^{1:i},a^{1:i}\right)\delta_1[i]\delta_k[t], \tag{35}$$

$$\begin{aligned}D_k^{\zeta}\left(t,x^{1:i},a^{1:i}\right) &= p_{S,k}\left(x^{i-1}\right)f\left(x^i|x^{i-1},a^{i-1}\right)g\left(a^i|a^{i-1}\right)\\ &\quad\times D_{k-1}\left(t,x^{1:i-1},a^{1:i-1}\right).\end{aligned} \tag{36}$$

We only consider alive trajectories, so the PHD $D_k^{\zeta}(\cdot)$ in (36) is zero if $t+i-1\neq k$. The proof of Proposition 1 can be found in Appendix A. The proof of the KLD minimization is omitted, since the trajectory augmented with the detection probability sequence is a simple extension of the classical trajectory state, and the proof of the latter can be found in [32].

Remark 1: The robust PHD filter [38] only considers the target state and corresponding detection probability at the current time. In contrast, in Proposition 1, the past states of the trajectory and detection profile sequence are kept in the U-TPHD filter. The condition also applies to the prediction step in the U-TCPHD filter following.

Proposition 2: If at time k, the predicted PHD $D_{k|k-1}(\tilde{X})$ is given, then the posterior PHD $D_k(\tilde{X})$ is given by

$$\begin{aligned}&D_k\left(t,x^{1:i},a^{1:i}\right)\\ &= D_{k|k-1}\left(t,x^{1:i},a^{1:i}\right)\left(1-a^i\right) + D_{k|k-1}\left(t,x^{1:i},a^{1:i}\right)a^i\end{aligned}$$

$$\times \sum_{z\in Z_k} \frac{l_k(z|x^i)}{\lambda_c \bar{c}(z) + \iint a^i \cdot l_k(z|x^i) D^{\tau}_{k|k-1}(x^i,a^i) da^i dx^i}, \tag{37}$$

where

$$D^{\tau}_{k|k-1}(x^i,a^i) = \sum_{t=1}^{k} \iint D_{k|k-1}(t, x^{1:k-t+1}, a^{1:k-t+1}) \times dx^{1:k-t} da^{1:k-t}, \tag{38}$$

with $i = k - t + 1$.

In Proposition 2, the PHD of the prior density of augmented targets at time k is expressed as $D^{\tau}_{k|k-1}(x^i, a^i)$, which is obtained by the marginalization for the PHD of augmented multi-trajectory densities. The marginalization step is also applied to the U-TCPHD filter. The proof of Proposition 2 is detailed in Appendix B.

Remark 2: Different from the TPHD filter [32], which only considers the PHD of trajectory, the updated PHD in the U-TPHD filter contains information about both the trajectory $X = (t, x^{1:i})$ and detection probability sequence $A = a^{1:i}$. The detection profile sequence A and the trajectory X are mutually coupled. If we obtain a better estimation of the detection profile sequence, then the trajectory estimation will also be influenced.

C. The U-TCPHD Filter

In this section, the recursion of the U-TCPHD filter is derived in detail. The U-TCPHD propagates the augmented multi-trajectory density of an IID cluster RFS. In the prediction and update steps, the U-TCPHD filter uses the KLD minimization to obtain the best IID cluster approximation [21]. Based on this theory, it propagates the PHD of an IID cluster augmented multi-trajectory density and the cardinality distribution. The following propositions show recursion steps of the U-TCPHD filter.

Based on Assumptions 1, 2, and 3, the recursion of the U-TCPHD filter also follows the routine of:

Assumption 5: The clutter is IID cluster and independent of target generated measurements, with the cardinality distribution $\rho_{c,k}$. Besides, the cardinality distribution of new born trajectories is given as $\rho_{\gamma,k}$.

Assumption 6: Both the prior and posterior augmented multi-trajectory densities are IID cluster through the KLD minimization.

Proposition 3: If at time $k-1$, the posterior PHD $D_{k-1}(\cdot)$ and posterior cardinality distribution $\rho_{k-1}(\cdot)$ are given, then the predicted PHD $D_{k|k-1}(\cdot)$ for $\tilde{X} = (t, x^{1:i}, a^{1:i})$ and predicted cardinality distribution $\rho_{k|k-1}$ are given as

$$D_{k|k-1}\left(\tilde{X}\right) = \gamma_k\left(\tilde{X}\right) + D^{\zeta}_k\left(\tilde{X}\right), \tag{39}$$

$$\rho_{k|k-1}(n) = \sum_{j=0}^{n} \rho_{\gamma,k}(n-j) \sum_{\ell=j}^{\infty} C^{\ell}_j \rho_{k-1}(\ell) \times \left[\iint \left(1 - p_{S,k}(x^{i-1})\right) D^{\tau}_{k-1}(x^{i-1}, a^{i-1}) da^{i-1} dx^{i-1}\right]^{\ell-j} \times \frac{\left[\iint p_{S,k}(x^{i-1}) D^{\tau}_{k-1}(x^{i-1}, a^{i-1}) da^{i-1} dx^{i-1}\right]^{j}}{\left[\iint D^{\tau}_{k-1}(x^{i-1}, a^{i-1}) da^{i-1} dx^{i-1}\right]^{\ell}}. \tag{40}$$

where

$$D^{\tau}_{k-1}(x^{i-1}, a^{i-1}) = \sum_{t=1}^{k-1} \iint D_{k-1}(t, x^{1:i-1}, a^{1:i-1}) \times dx^{1:i-2} da^{1:i-2}, \tag{41}$$

Proposition 4: If at time k, the predicted PHD $D_{k|k-1}(\tilde{X})$ and predicted cardinality distribution $\rho_{k|k-1}$ are given, where $\tilde{X} = (t, x^{1:i}, a^{1:i})$, then the posterior PHD D_k and posterior cardinality distribution ρ_k are given as

$$D_k\left(t, x^{1:i}, a^{1:i}\right) = D_{k|k-1}\left(t, x^{1:i}, a^{1:i}\right)(1 - a^i) \times \frac{\left\langle \Upsilon^1_k\left[D^{\tau}_{k|k-1}; Z_k\right], \rho_{k|k-1}\right\rangle}{\left\langle \Upsilon^0_k\left[D^{\tau}_{k|k-1}; Z_k\right], \rho_{k|k-1}\right\rangle} + D_{k|k-1}\left(t, x^{1:i}, a^{1:i}\right) a^i \sum_{z\in Z_k} \frac{l_k\left(z|x^i\right)}{\bar{c}(z)} \times \frac{\left\langle \Upsilon^1_k\left[D^{\tau}_{k|k-1}; Z_k \backslash \{z\}\right], \rho_{k|k-1}\right\rangle}{\left\langle \Upsilon^0_k\left[D^{\tau}_{k|k-1}; Z_k\right], \rho_{k|k-1}\right\rangle}, \tag{42}$$

$$\rho_k(n) = \frac{\Upsilon^0_k\left[D^{\tau}_{k|k-1}; Z_k\right](n) \rho_{k|k-1}(n)}{\left\langle \Upsilon^0_k\left[D^{\tau}_{k|k-1}; Z_k\right], \rho_{k|k-1}\right\rangle}, \tag{43}$$

where

$$\Upsilon^u_k\left[D^{\tau}_{k|k-1}, Z_k\right](n) = \sum_{j=0}^{\min(|Z_k|, n-u)} (|Z_k| - j)! \rho_{c,k}(|Z_k| - j) \times P^n_{j+u} e_j\left(\Xi\left(D^{\tau}_{k|k-1}, Z_k\right)\right) \times \frac{\left[\iint (1 - a^i) D^{\tau}_{k|k-1}(x^i, a^i) da^i dx^i\right]^{n-j-u}}{\left[\iint D^{\tau}_{k|k-1}(x^i, a^i) da^i dx^i\right]^{n}}, \tag{44}$$

$$\Xi\left(D^{\tau}_{k|k-1}, Z_k\right) = \left\{\iint a^i \cdot \frac{l_k\left(z|x^i\right)}{\bar{c}(z)} D^{\tau}_{k|k-1}\left(x^i, a^i\right) da^i dx^i : z \in Z_k\right\}. \tag{45}$$

In Proposition 3, the notation D^{τ}_{k-1} represents the PHD of the posterior density of augmented targets at time $k-1$, which can be obtained by (38). In Proposition 4, the updated cardinality $\rho_k(\cdot)$ incorporates the clutter cardinality, the measurement set, the prior PHD and predicted cardinality distribution. It should be noted that at each recursion step, the cardinality distribution for a set of augmented trajectories is the same as that for a set of targets. Therefore, the update of cardinality distribution in the U-TCPHD filter and the classic CPHD filter [14] share similar principles. The proof of Proposition 4 can be found in Appendix C.

D. Possible Extension

Similarly, the U-TPHD filter can be also extended to consider the unknown clutter rate [38]. In this situation, the hybrid augmented trajectory space model is given as $\mathbb{Y} = \mathbb{U} \uplus (\mathbb{C} \times \mathbb{D})$, where $\mathbb{C}$ and $\mathbb{D}$ denote the state space of clutter c and its detection probability o, respectively. It is assumed that trajectories and clutter generators are statistically independent. The integral function of the density $\bar{p}(\cdot)$ of a single hybrid augmented trajectory $\tilde{X}_c \in \mathbb{Y}$ is given as

$$\int_{\mathbb{Y}} \bar{p}\left(\tilde{X}_c\right) d\tilde{X}_c = \sum_{(t,i)\in\mathbb{I}} \int_{\mathbb{R}^{in_x}} \int_{\mathbb{D}^i} \bar{p}\left(t, x^{1:i}, a^{1:i}\right) da^{1:i} dx^{1:i} + \int_{\mathbb{C}} \int_{\mathbb{D}} \bar{p}(c, o) dc do. \tag{46}$$

Let $D_k(c, o)$ denote the PHD of the clutter generators, $p^c_{S,k}$ denote survival probability and $\gamma_k(c, o)$ denote PHD of the birth clutter from clutter generators at time k. Using the same principle and assumptions of [38], the recursion of the new U-TPHD filter is given as

$$D_{k|k-1}\left(\tilde{X}\right) = \gamma_k\left(\tilde{X}\right) + D^{\zeta}_k\left(\tilde{X}\right), \tag{47}$$

$$D_{k|k-1}(c, o) = \gamma_k(c, o) + p^c_{S,k} D_{k-1}(c, o), \tag{48}$$

$$D_k\left(\tilde{X}\right) = D_{k|k-1}\left(\tilde{X}\right)(1 - a^i) + D_{k|k-1}\left(\tilde{X}\right) a^i \sum_{z\in Z_k} \frac{l_k(z|x^i)}{\Theta_k\left[z, c, o, \tilde{x}\right]}, \tag{49}$$

$$D_k(c, o) = D_{k|k-1}(c, o)(1 - o) + D_{k|k-1}(c, o) o \sum_{z\in Z_k} \frac{\bar{c}_k(z)}{\Theta_k\left[z, c, o, \tilde{x}\right]}, \tag{50}$$

where

$$\Theta_k\left[z, c, o, \tilde{x}\right] = \iint o \cdot \bar{c}(z) D_{k|k-1}(c, o) dc do + \iint a^i \cdot l_k(z|x^i) D^{\tau}_{k|k-1}(x^i, a^i) da^i dx^i. \tag{51}$$

The extension of the U-TCPHD filter also propagates the cardinality distribution of the hybrid augmented trajectory. The specific derivation of the U-TCPHD filter considering both unknown clutter rate and detection probability is a similar development to the U-TPHD filter. In this paper, we focus on the derivation of unknown detection probability, hence their implementation methods considering clutter rate are omitted in this paper. Further details about unknown clutter rate can be found in [38].

IV. Beta-Gaussian Mixture Implementation for the U-TPHD and U-TCPHD Filters

In this section, the closed form implementations for the U-TPHD and U-TCPHD filters immune to the unknown detection profile are derived respectively. In Section IV-A, the reason of simplifying both filters to consider the detection profile only at a single frame time is discussed. In Section IV-B, the Beta-Gaussian mixture implementations [38] are presented for the U-TPHD and U-TCPHD filters, which are referred to as the BG-U-TPHD and BG-U-TCPHD filters. In Section IV-C, the L-scan approximations of the BG-U-TPHD and BG-U-TCPHD filters are presented to reduce the computational burden. The estimation step is given in Section IV-D.

A. Only Current Detection Profile

It can be seen from the Propositions 1–4 that the U-TPHD and U-TCPHD filters update the PHD of augmented trajectories in recursions, which considers the information about the sequence of unknown detection profile. In this section, we advocate for only considering the unknown detection profile at the current time for simplicity.

Regarding the algorithmic efficiency, the computational cost rises significantly with the increasing length of the trajectory and the sequence of detection probabilities. For simplicity, we only consider P discrete probability values to describe the detection probability distribution, which are the uniform grids of interval [0, 1]. Then, as indicated by (36), for a certain surviving trajectory $X = (t, x^{1:i-1})$ at time $k - 1$, its historical detection probability space contains P^{i-1} components, and the number of components will increase to P^i at time k. In other words, the computational burden of a single trajectory with length l is $\mathcal{O}(P^l)$, which is not acceptable in the implementation.

Therefore, in consideration of the algorithmic efficiency, we propose to consider the effect of the unknown detection probability at the current time for the implementations of the U-TPHD and U-TCPHD filters. In [38], the Beta-Gaussian mixture provides an efficient method to directly describe the unknown detection probability, and this method can be also adopted for the U-TPHD and U-TCPHD filters. For similarity, the unknown detection probability only at the current time is considered in the implementation. Based on this condition, the transition density $f(\cdot|\cdot)$ of targets in (31) is assumed to be independent of the detection probability. Thus, the augmented trajectory in (28) becomes $\tilde{X} = (t, x^{1:i}, a^i)$ and the prediction of augmented trajectory PHD (34) can be written as

$$D_{k|k-1}\left(t, x^{1:i}, a^i\right) = \gamma\left(t, x^{1:i}, a^i\right) \delta_1[i]\delta_k[t] + p_{S,k}\left(x^{i-1}\right) f\left(x^i|x^{i-1}\right) \times \int g\left(a^i|a^{i-1}\right) D_{k-1}\left(t, x^{1:i-1}, a^{i-1}\right) da^{i-1}. \tag{52}$$

Different from (36) and (39), the past states of the detection probability sequence are not retained in the predicted PHD and both filters only update the information regarding detection probability at the current time. After marginalization, the PHD of the augmented target in (38) can be computed as

$$D^{\tau}_{k|k-1}(x^i, a^i) = \sum_{t=1}^{k} \int D_{k|k-1}(t, x^{1:k-t+1}, a^i) dx^{1:k-t}, \quad (53)$$

with $i = k - t + 1$. The change of (38) applies to (37), (40), (42) and (43).

B. The BG-U-TPHD and BG-U-TCPHD Filters

In this section, the closed form implementations are presented for the U-TPHD and U-TCPHD filters by using the Beta-Gaussian mixtures [38]. At time k, the Gaussian density of the trajectory born at time t with length of i is denoted as [32]

$$\mathcal{N}(t, x^{1:i}; t^k, \widehat{m}^k, \widehat{P}^k) = \mathcal{N}(x^{1:i}; \widehat{m}^k, \widehat{P}^k)\delta_{[t^k]}[t]\delta_{[i_k]}[i]. \quad (54)$$

where $\widehat{m}^k \in \mathbb{R}^{in_x}$ and $\widehat{P}^k \in \mathbb{R}^{in_x \times in_x}$ denote, respectively, the mean and covariance. The term $t^k = k - i_k + 1$ denotes the birth time. The length of trajectory satisfies $i_k = \dim(\widehat{m}^k/n_x)$. For a matrix V, the notation $V_{[n:m,s:t]}$ represents the submatrix of V for rows from time steps n to m and columns from time steps s to t. The notation $V_{[n:m]}$ is used to present the submatrix of V for rows from time steps n to m. Besides, the notations $V_{[n,s:t]}$ and $V_{[n]}$ represent $V_{[n:n,s:t]}$ and $V_{[n:n]}$, respectively.

The PDF of a Beta distribution is given as

$$\beta(y; u, v) = \frac{y^{u-1}(1-y)^{v-1}}{\int_0^1 y^{u-1}(1-y)^{v-1} dy}, \quad (55)$$

where the denominator $\int_0^1 y^{u-1}(1-y)^{v-1}dy$ denotes the Beta function $B(u, v)$ and the parameters u and v should satisfy $u > 1, v > 1$. Some properties of the Beta distribution are summarized as follows [38],

$$(1-y)\beta(y; u, v) = \frac{v}{u+v}\beta(y; u, v+1), \quad (56)$$

$$y\beta(y; u, v) = \frac{u}{u+v}\beta(y; u+1, v). \quad (57)$$

The transition density for the detection probability in (52) is given as

$$g\left(a^i | a^{i-1}\right) = \beta\left(a; u^{k|k-1}, v^{k|k-1}\right), \quad (58)$$

where

$$a^i = a = \frac{u^{k|k-1}}{u^{k|k-1} + v^{k-1}}, \quad (59)$$

$$u^{k|k-1} = \left(\frac{\mu^{k|k-1}\left(1-\mu^{k|k-1}\right)}{\left[\sigma^{k|k-1}\right]^2} - 1\right)\mu^{k|k-1}, \quad (60)$$

$$v^{k|k-1} = \left(\frac{\mu^{k|k-1}\left(1-\mu^{k|k-1}\right)}{\left[\sigma^{k|k-1}\right]^2} - 1\right)\left(1-\mu^{k|k-1}\right), \quad (61)$$

$$\mu^{k|k-1} = \frac{u^{k-1}}{u^{k-1} + v^{k-1}} = a^{i-1}, \quad (62)$$

$$\left[\sigma^{k|k-1}\right]^2 = |k_\beta| \frac{u^{k-1}v^{k-1}}{\left(u^{k-1}+v^{k-1}\right)^2\left(u^{k-1}+v^{k-1}+1\right)}, \quad (63)$$

with $|k_\beta|$ is a constant slightly bigger than 1.

1) The BG-U-TPHD Filter: there are some assumptions given as follows.

Assumption 7: The target kinematics and observation models are given as the linear Gaussian model [32]

$$f\left(x^i | x^{i-1}\right) = \mathcal{N}\left(x^i; Fx^{i-1}, Q\right), \quad (64)$$

$$l\left(z | x^i\right) = \mathcal{N}\left(z; Hx^i, R\right), \quad (65)$$

where $F \in \mathbb{R}^{n_x \times n_x}$ denotes the state transition matrix, $Q \in \mathbb{R}^{n_x \times n_x}$ is the process noise covariance, $H \in \mathbb{R}^{n_z \times n_x}$ is the observation matrix and $R \in \mathbb{R}^{n_z \times n_z}$ denotes the observation noise covariance.

Assumption 8: To simplify this model, the survival probability is taken as a constant.

Assumption 9: The PHD of birth density is given as

$$\gamma_k\left(\tilde{X}\right) = \sum_{j=1}^{J^k_\gamma} \omega^k_{\gamma,j}\beta\left(a; u^k_{\gamma,j}, v^k_{\gamma,j}\right)\mathcal{N}\left(X; k, \widehat{m}^k_{\gamma,j}, \widehat{P}^k_{\gamma,j}\right), \quad (66)$$

where J^k_γ denotes the number of new born trajectories. For the j-th birth component at time k, $\omega^k_{\gamma,j}$ represents the weight. The mean and covariance of the Gaussian density of the trajectory born at time k are expressed as $\widehat{m}^k_{\gamma,j} \in \mathbb{R}^{n_x}$ and $\widehat{P}^k_{\gamma,j} \in \mathbb{R}^{n_x \times n_x}$, respectively. The terms $u^k_{\gamma,j}$ and $v^k_{\gamma,j}$ denote the corresponding factors of the Beta distribution.

Proposition 5: If at time $k-1$, the posterior PHD D_{k-1} is given and D_{k-1} is a Beta-Gaussian mixture of the form

$$D_{k-1}\left(\underline{\tilde{X}}\right) = \sum_{j=1}^{J^{k-1}} \omega^{k-1}_j \beta\left(a; u^{k-1}_j, v^{k-1}_j\right) \times \mathcal{N}\left(X; t^{k-1}_j, \widehat{m}^{k-1}_j, \widehat{P}^{k-1}_j\right) \quad (67)$$

where, at time $k-1$, the length of the j-th trajectory is $i^{k-1}_j = k - t^{k-1}_j$. The mean and covariance of the Gaussian density are given as $\widehat{m}^{k-1}_j \in \mathbb{R}^{i^{k-1}_j n_x}$ and $\widehat{P}^{k-1}_j \in \mathbb{R}^{i^{k-1}_j n_x \times i^{k-1}_j n_x}$, respectively. Thus, the prior PHD $D_{k|k-1}$ is given as

$$\begin{aligned} D_{k|k-1}\left(\tilde{X}\right) = &\sum_{j=1}^{J^k_\gamma} \omega^k_{\gamma,j}\beta\left(a; u^k_{\gamma,j}, v^k_{\gamma,j}\right) \\ &\times \mathcal{N}\left(X; k, \widehat{m}^k_{\gamma,j}, \widehat{P}^k_{\gamma,j}\right) \\ &+ p_s \sum_{j=1}^{J^{k-1}} \omega^{k-1}_j \beta\left(a; u^{k|k-1}_{S,j}, v^{k|k-1}_{S,j}\right) \\ &\times \mathcal{N}\left(X; t^{k|k-1}_{S,j}, \widehat{m}^{k|k-1}_{S,j}, \widehat{P}^{k|k-1}_{S,j}\right), \end{aligned} \quad (68)$$

where

$$\widehat{m}^{k|k-1}_{S,j} = \left[\left[\widehat{m}^{k-1}_j\right]^\top, \left[F \cdot \widehat{m}^{k-1}_{j,[k-1]}\right]^\top\right]^\top, \quad (69)$$

$$\widehat{P}^{k|k-1}_{S,j} = \begin{bmatrix} \widehat{P}^{k-1}_j & P_1 \\ P_1^\top & P_2 \end{bmatrix}, \quad (70)$$

$$P_1 = \widehat{P}^{k-1}_{j,\left[t_j^{k-1}:k-1,k-1\right]} F^\top, \tag{71}$$

$$P_2 = F \widehat{P}^{k-1}_{j,[k-1,k-1]} F^\top + Q. \tag{72}$$

The prediction of each Beta-Gaussian component is obtained by the prediction of the Beta part (denoting the detection probability) multiplied by the prediction of the Gaussian part (denoting the trajectory). Compared to the prediction step in the GM-TPHD filter [32], the prediction of trajectory in the BG-U-TPHD filter still roots in the transition of the target kinematic state, while the prediction of detection probability is completely governed by Beta densities. The notation $t_S^{k|k-1}$ denotes the birth time of the surviving trajectory.

Proposition 6: If at time k, the prior PHD $D_{k|k-1}$ is given, which is a Beta-Gaussian mixture of the form

$$D_{k|k-1}\left(\tilde{X}\right) = \sum_{j=1}^{J^{k|k-1}} \omega_j^{k|k-1} \beta\left(a; u_j^{k|k-1}, v_j^{k|k-1}\right) \times \mathcal{N}\left(X; t_j^{k|k-1}, \widehat{m}_j^{k|k-1}, \widehat{P}_j^{k|k-1}\right). \tag{73}$$

Then, given a measurement set Z_k, the posterior PHD D_k is given as

$$\begin{aligned} D_k\left(\tilde{X}\right) = &\sum_{j=1}^{J^{k|k-1}} \omega_j^{v,k} \beta\left(a; u_j^{k|k-1}, v_j^{k|k-1}+1\right) \\ &\times \mathcal{N}\left(X; t_j^{k|k-1}, \widehat{m}_j^{k|k-1}, \widehat{P}_j^{k|k-1}\right) \\ &+ \sum_{z\in Z_k} \sum_{j=1}^{J^{k|k-1}} \omega_j^{u,k}(z) \beta\left(a; u_j^{k|k-1}+1, v_j^{k|k-1}\right) \\ &\times \mathcal{N}\left(X; t_j^{k}, \widehat{m}_j^{k}(z), \widehat{P}_j^{k}\right), \end{aligned} \tag{74}$$

where

$$\omega_j^{v,k} = \omega_j^{k|k-1} \frac{B\left(u_j^{k|k-1}, v_j^{k|k-1}+1\right)}{B\left(u_j^{k|k-1}, v_j^{k|k-1}\right)}, \tag{75}$$

$$\begin{aligned} \omega_j^{u,k} = &\omega_j^{k|k-1} \frac{B\left(u_j^{k|k-1}+1, v_j^{k|k-1}\right)}{B\left(u_j^{k|k-1}, v_j^{k|k-1}\right)} \\ &\times \frac{q_j(z)}{\lambda_c \bar{c}(z) + \sum_{l=1}^{J_{k|k-1}} \frac{u_l^{k|k-1}}{u_l^{k|k-1}+v_l^{k|k-1}} \omega_l^{k|k-1} q_l(z)}, \end{aligned} \tag{76}$$

$$\bar{z}_j = H \widehat{m}_{j,[k]}^{k|k-1}, \tag{77}$$

$$S_j = H \widehat{P}^{k|k-1}_{j,[k,k]} H^\top + R, \tag{78}$$

$$q_j(z) = \mathcal{N}\left(z; \bar{z}_j, S_j\right), \tag{79}$$

$$\widehat{m}_j^k(z) = \widehat{m}_j^{k|k-1} + K_j\left(z - \bar{z}_j\right), \tag{80}$$

$$\widehat{P}_j^k = \widehat{P}_j^{k|k-1} - K_j H \widehat{P}^{k|k-1}_{j,[k,t_j^{k|k-1}:k]}, \tag{81}$$

$$K_j = \widehat{P}^{k|k-1}_{j,[t_j^{k|k-1}:k,k]} H^\top S_j^{-1}. \tag{82}$$

The BG-U-TPHD filter also adopts the Kalman filter in the update step, but aims at the whole trajectory. It not only updates the estimation of the target state at the current time, but also smooths the estimation of the previous states. Different from the GM-TPHD filter [32], the updated detection probabilities can be obtained by the number of measurements associated with trajectories.

2) The BG-U-TCPHD Filter: based on Assumptions 5, 6, 7, 8, and 9, the recursion of the BG-U-TCPHD filter is obtained by the following propositions

Proposition 7: If at time $k-1$, the posterior PHD D_{k-1} and posterior cardinality distribution ρ_{k-1} are given, where D_{k-1} is a Beta-Gaussian mixture of the form

$$D_{k-1}\left(\underline{\tilde{X}}\right) = \sum_{j=1}^{J^{k-1}} \omega_j^{k-1} \beta\left(a; u_j^{k-1}, v_j^{k-1}\right) \times \mathcal{N}\left(X; t_j^{k-1}, \widehat{m}_j^{k-1}, \widehat{P}_j^{k-1}\right). \tag{83}$$

Then at time k, the prior cardinality distribution $\rho_{k|k-1}$ and PHD $D_{k|k-1}$ are given as

$$\rho_{k|k-1}(n) = \sum_{j=0}^{n} \rho_{\gamma,k}(n-j) \sum_{\ell=j}^{\infty} C_j^\ell \rho_{k-1}(\ell) \times {p_{S,k}}^j \left(1-p_{S,k}\right)^{\ell-j}, \tag{84}$$

$$\begin{aligned} D_{k|k-1}\left(\tilde{X}\right) = &\sum_{j=1}^{J_\gamma^k} \omega_{\gamma,j}^k \beta\left(a; u_{\gamma,j}^k, v_{\gamma,j}^k\right) \mathcal{N}\left(X; k, \widehat{m}_{\gamma,j}^k, \widehat{P}_{\gamma,j}^k\right) \\ &+ p_{S,k} \sum_{j=1}^{J^{k-1}} \omega_j^{k-1} \beta\left(a; u_{S,j}^{k|k-1}, v_{S,j}^{k|k-1}\right) \\ &\times \mathcal{N}\left(X; t_{S,j}^{k|k-1}, \widehat{m}_{S,j}^{k|k-1}, \widehat{P}_{S,j}^{k|k-1}\right). \end{aligned} \tag{85}$$

In Proposition 7, the derivation of the prior PHD is the same as the BG-U-TPHD filter, which retains previous states of trajectories, while the BG-U-TCPHD filter also contains the prediction of cardinality distribution.

Proposition 8: If at time k, the prior PHD $D_{k|k-1}$ is given, which is a Beta-Gaussian mixture of the form

$$D_{k|k-1}\left(\tilde{X}\right) = \sum_{j=1}^{J^{k|k-1}} \omega_j^{k|k-1} \beta\left(a; u_j^{k|k-1}, v_j^{k|k-1}\right) \times \mathcal{N}\left(X; t_j^{k|k-1}, \widehat{m}_j^{k|k-1}, \widehat{P}_j^{k|k-1}\right). \tag{86}$$

By receiving a set of measurements Z_k, the cardinality distribution ρ_k and the posterior PHD D_k at time k can be obtained as follows,

$$D_k\left(\tilde{X}\right) = \sum_{j=1}^{J^{k|k-1}} \omega_j^{v,k} \beta\left(a; u_j^{k|k-1}, v_j^{k|k-1}+1\right) \tag{87}$$

$$\times \mathcal{N}\left(X; t_j^{k|k-1}, \widehat{m}_j^{k|k-1}, \widehat{P}_j^{k|k-1}\right)$$
$$+ \sum_{z \in Z_k} \sum_{j=1}^{J^{k|k-1}} \omega_j^{u,k}(z) \beta\left(a; u_j^{k|k-1}+1, v_j^{k|k-1}\right)$$
$$\times \mathcal{N}\left(X; t_j^k, \widehat{m}_j^k(z), \widehat{P}_j^k\right),$$

$$\rho_k(n) = \frac{\Upsilon_k^0\left[a^{k|k-1}, \omega^{k|k-1}, Z_k\right](n)\rho_{k|k-1}(n)}{\left\langle \Upsilon_k^0\left[a^{k|k-1}, \omega^{k|k-1}, Z_k\right], \rho_{k|k-1}\right\rangle}, \tag{88}$$

where

$$\Upsilon^u\left[a^{k|k-1}, \omega^{k|k-1}, Z_k\right](n)$$
$$= \sum_{j=0}^{\min(|Z_k|, n-u)} (|Z_k|-j)!\rho_c\left(|Z_k|-j\right) P_{j+u}^n \tag{89}$$
$$\times \frac{\left\langle 1-a^{k|k-1}, \omega^{k|k-1}\right\rangle^{n-j-u}}{\left\langle 1, \omega^{k|k-1}\right\rangle^n}$$
$$\times e_j\left(\Lambda_k\left(a^{k|k-1}, \omega^{k|k-1}, Z_k\right)\right),$$

$$\Lambda_k\left(a^{k|k-1}, \omega^{k|k-1}, Z_k\right)$$
$$= \left\{\sum_{j=1}^{J^{k|k-1}} a_j^{k|k-1} \frac{q(z)}{\bar{c}(z)} \omega_j^{k|k-1} : z \in Z_k\right\}, \tag{90}$$

$$\omega^{k|k-1} = \left[\omega_1^{k|k-1}, \ldots, \omega_{J^{k|k-1}}^{k|k-1}\right]^\top, \tag{91}$$

$$a^{k|k-1} = \left[\frac{u_1^{k|k-1}}{u_1^{k|k-1}+v_1^{k|k-1}}, \ldots, \frac{u_{J^{k|k-1}}^{k|k-1}}{u_{J^{k|k-1}}^{k|k-1}+v_{J^{k|k-1}}^{k|k-1}}\right]^\top, \tag{92}$$

$$q(z) = [q_1(z), \ldots, q_{J^{k|k-1}}(z)]^{\mathrm{T}}, \tag{93}$$

$$\omega_j^{v,k} = \omega_j^{k|k-1} \frac{B\left(u_j^{k|k-1}, v_j^{k|k-1}+1\right)}{B\left(u_j^{k|k-1}, v_j^{k|k-1}\right)} \tag{94}$$
$$\times \frac{\left\langle \Upsilon_k^1\left[a^{k|k-1}, \omega^{k|k-1}, Z_k\right], \rho_{k|k-1}\right\rangle}{\left\langle \Upsilon_k^0\left[a^{k|k-1}, \omega^{k|k-1}, Z_k\right], \rho_{k|k-1}\right\rangle},$$

$$\omega_j^{u,k} = \omega_j^{k|k-1} \frac{B\left(u_j^{k|k-1}+1, v_j^{k|k-1}\right)}{B\left(u_j^{k|k-1}, v_j^{k|k-1}\right)}$$
$$\times \frac{\left\langle \Upsilon_k^1\left[a^{k|k-1}, \omega^{k|k-1}, Z_k \backslash \{z\}\right], \rho_{k|k-1}\right\rangle}{\left\langle \Upsilon_k^0\left[a^{k|k-1}, \omega^{k|k-1}, Z_k\right], \rho_{k|k-1}\right\rangle} \frac{q_j(z)}{\bar{c}(z)}. \tag{95}$$

Proposition 8 shows that the BG-U-TCPHD filter updates not only trajectories and detection probabilities, but also the cardinality distribution. To limit unbounded Beta-Gaussian components in the BG-U-TPHD and BG-U-TCPHD filters, the pruning and absorption steps for mixture components are proposed, and the detail steps are given in Table I.

TABLE I
THE ALGORITHM FOR PRUNING AND ABSORPTION

Give posterior PHD parameters $\{\Phi_j^k\}_{j=1}^{J_k}$, which equal to $\left\{\omega_j^k, t_j^k, i_j^k, \widehat{m}_j^k, \widehat{P}_j^k, u_j^k, v_j^k\right\}_{j=1}^{J^k}$, a pruning threshold T_p, a absorption threshold T_a and maximum allowable number of Gaussian terms J_{max}. Set $\ell = 0$ and $\Theta = \left\{i = 1, ..., J^k \mid \omega_i^k > T_p\right\}$.
Loop
$\ell = \ell + 1$.
$j = \underset{i \in \Theta}{argmax}\, \omega_i^k$.
$L = \{i \in \Theta : (\widehat{m}_{i,[k]}^k - \widehat{m}_{j,[k]}^k)^\top (\widehat{P}_{j,[k,k]}^k)^{-1} (\widehat{m}_{i,[k]}^k - \widehat{m}_{j,[k]}^k) \leq T_a\}$.
$\bar{\omega}_\ell^k = \sum_{i \in L} \omega_i^k$,
$\mu_i^k = \frac{u_i^k}{u_i^k + v_i^k}$,
$\left[\sigma_i^k\right]^2 = \frac{u_i^k v_i^k}{(u_i^k+v_i^k)^2 (u_i^k+v_i^k+1)}$,
$\bar{\mu}^k = \frac{1}{\bar{\omega}_\ell^k} \sum_{i \in L} \omega_i^k \mu_i^k$,
$\left[\bar{\sigma}^k\right]^2 = \frac{1}{\bar{\omega}_\ell^k} \sum_{i \in L} \omega_i^k \left[\sigma_i^k\right]^2$,
$u_\ell^k = \left(\frac{\bar{\mu}^k\left(1-\bar{\mu}^k\right)}{\left[\bar{\sigma}^k\right]^2} - 1\right) \bar{\mu}^k$,
$v_\ell^k = \left(\frac{\bar{\mu}^k\left(1-\bar{\mu}^k\right)}{\left[\bar{\sigma}^k\right]^2} - 1\right) \left(1 - \bar{\mu}^k\right)$,
$\bar{\Phi}_\ell^k = \Phi_j^k$ with weight $\bar{\omega}_\ell^k$ and Beta distribution factors u_ℓ^k, v_ℓ^k.
$\Theta = \Theta \backslash L$.
If $\Theta = \emptyset$, **break**
if $\ell > J_{max}$ then replace $\bar{\Phi}_\ell^k$ by the J_{max} Gaussian components with largest weights.
Output: $\{\bar{\Phi}_j^k\}_{j=1}^{min\{\ell, J_{max}\}}$.

It should be noted that, the absorption step is different from the merging step in the robust BG-CPHD filter [38]. In this paper, the absorption is that, for two closely spaced Beta-Gaussian components, only the weight and Beta distribution factors of the smaller one are added to the higher component. Because the distance of two Beta-Gaussian components are measured based on the target states at the current time, while their past trajectory states can be extremely different.

C. L-Scan Approximation

The L-scan approximation is proposed in [32] to reduce the computational burden brought by the increasing length of trajectory. This approximation is also applied to the BG-U-TPHD and BG-U-TCPHD filters, which only updates the augmented multi-trajectory density of the last L time and keeps the rest unaltered. The notation L is used to denote the value of the L-scan approximation. When the length of trajectory satisfy $i \leq L$, the prediction and update steps are the same as those in Section IV-B. However, when we have $i \geq L$, the prediction step changes to

$$\widehat{m}_j^{L,k|k-1} = \left[\left[\widehat{m}_{j,[2:L]}^{L,k-1}\right]^\top, \left[F \cdot \widehat{m}_{j,[L]}^{L,k-1}\right]^\top\right]^\top, \tag{96}$$

$$\widehat{P}_j^{L,k|k-1} = \begin{bmatrix} \widehat{P}_{j,[2:L,2:L]}^{L,k-1} & \widehat{P}_{j,[2:L,L]}^{L,k-1} F^\top \\ F\widehat{P}_{j,[L,2:L]}^{L,k-1} & F\widehat{P}_{j,[L,L]}^{L,k-1} F^\top + Q \end{bmatrix}, \tag{97}$$

where the mean $\widehat{m}^{L,k-1} \in \mathbb{R}^{Ln_x}$ and the covariance $\widehat{P}^{L,k-1} \in \mathbb{R}^{Ln_x \times Ln_x}$. The update step is given by

$$\bar{z}_j = H\widehat{m}_{j,[L]}^{L,k|k-1}, \tag{98}$$

$$S_j = H\widehat{P}_{j,[L,L]}^{L,k|k-1} H^\top + R, \tag{99}$$

$$\widehat{m}_j^{L,k}(z) = \widehat{m}_j^{L,k|k-1} + K_j\left(z - \bar{z}_j\right), \tag{100}$$

$$\widehat{P}_j^{L,k} = \widehat{P}_j^{L,k|k-1} - K_j H \widehat{P}_{j,[L,1:L]}^{L,k|k-1}, \tag{101}$$

$$K_j = \widehat{P}_{j,[1:L,L]}^{L,k|k-1} H^\top S_j^{-1}. \tag{102}$$

Besides, the matrix $A_j^k = \widehat{m}_{j,[t_j^k:k-L]}^k \in \mathbb{R}^{(i_j^k-L)n_x}$ is needed to store the trajectory outside the L-scan window, even if they are not updated. The intact trajectory information at the current time, consists of the contents in the matrix A and the corresponding L-scan window, which is written as $\widehat{m}_j^k = [[A_j^k]^\top, [\widehat{m}_j^{L,k}]^\top]^\top$. In other words, both filters will propagate $\widehat{m}^L$, A and $\widehat{P}^L$ instead of $\widehat{m}$ and $\widehat{P}$ by using the L-scan approximation. Meanwhile, in pruning and absorption procedures, the $\widehat{m}_j^k$ and $\widehat{P}_j^k$ in PHD parameter Φ_j^k are also replaced.The BG-U-TPHD and BG-U-TCPHD filters are equivalent to the robust BG-PHD and BG-CPHD filters [38] but keeping trajectory information. When the value of L equals to 1, the BG-U-TPHD and BG-U-TCPHD filtering recursion are analogous to the robust BG-PHD and BG-CPHD filtering recursions, but keeping the past means for each PHD component, which enables trajectory estimation.

D. Estimation of Trajectories and Detection Profile

In this section, we will elaborate on the estimation of a set of augmented trajectories at each time step in the BG-U-TPHD and BG-U-TCPHD filters. It should be noted that the estimation step is behind the pruning and absorption. For the BG-U-TPHD filter, the estimation of the number of alive trajectories at time k is given as

$$N^k = \text{round}\left(\sum_{j=1}^{J^k} \omega_j^k\right). \tag{103}$$

For the BG-U-TCPHD filter, the estimation of the number of alive trajectories at time k can be obtained as

$$N^k = \text{argmax}\rho_k\left(\cdot\right). \tag{104}$$

Then the estimated set of augmented trajectories is given as

$$\left\{\left(t_1,i_1^k,\widehat{m}_1^k,\frac{u_1^k}{u_1^k+v_1^k}\right),\ldots,\left(t_{N^k},i_{N^k}^k,\widehat{m}_{N^k}^k,\frac{u_{N^k}^k}{u_{N^k}^k+v_{N^k}^k}\right)\right\}, \tag{105}$$

which is applied to both proposed filters.

TABLE II
THE INITIAL TARGET STATES

	Kinematic State	Birth Time/s	Death Time/s
Target 1	$[1005, 1489, 8, -10]^\top$	1	100
Target 2	$[-256, 1011, 20, 3]^\top$	10	100
Target 3	$[-1507, 257, 11, 10]^\top$	10	100
Target 4	$[-1500, 250, 43, 0]^\top$	10	66
Target 5	$[246, 735, 15, 5]^\top$	20	80
Target 6	$[-243, 993, -6, -12]^\top$	40	100
Target 7	$[1000, 1500, 1, -10]^\top$	40	100
Target 8	$[250, 750, -45, 10]^\top$	40	80
Target 9	$[1000, 1500, -50, 0]^\top$	60	100
Target 10	$[250, 750, -40, 25]^\top$	60	100

V. Simulation Results

This section presents numerical studies for the BG-U-TPHD and BG-U-TCPHD filters. In Section V-A, we compare four kinds of filters, namely, the BG-U-TPHD, BG-U-TCPHD, GM-TPHD and GM-TCPHD filters, where the GM-TPHD and GM-TCPHD filters are with known detection probabilities [32]. At a further step, we compare the BG-U-TPHD and BG-U-TCPHD filters with different L. In Section V-B, we present the performance of the BG-U-TPHD and BG-U-TCPHD filters with lower detection probabilities, as well as their performance under the condition of an uneven and time-varying detection profile. All filters in this section are based on the L-scan approximation.

A. Scenario 1

Ten targets are simulated inside of a two-dimensional space with the size of $[-2000, 2000]\text{m} \times [0, 2000]\text{m}$ for 100 seconds. The target state matrix is given as $x = [p_x, p_y, \dot{p}_x, \dot{p}_y]^\top$ including the position (with unit: m) and velocity information (with unit: m/s). The observation matrix $z = [z_x, z_y]^\top$ includes the position information. The single target transition model is given as

$$F = \begin{bmatrix} I_2 & I_2\delta t \\ 0_2 & I_2 \end{bmatrix} \qquad Q = \sigma_v^2 \begin{bmatrix} \frac{\delta t^4}{4} I_2 & \frac{\delta t^3}{2} I_2 \\ \frac{\delta t^3}{2} I_2 & \delta t^2 I_2 \end{bmatrix}$$

$$H = \begin{bmatrix} I_2 & 0_2 \end{bmatrix} \qquad R = \sigma_\varepsilon^2 I_2$$

where I_2 represents the 2×2 unit matrix, 0_2 represents the 2×2 zero matrix, $\sigma_v^2 = 1\text{ms}^{-2}$, $\sigma_\varepsilon^2 = 2\text{ms}^{-2}$, and $\delta t = 1\,s$ denotes the sampling period. The survival probability is given as a constant $p_S = 0.99$. The detection probability is unknown and given as $p_D = 0.98$ in this subsection. The number of clutter per scan is Poisson distributed with mean of $\lambda_c = 20$, and uniformly distributed in region $S = [-2000, 2000]\text{m} \times [0, 2000]\text{m}$. The value of clutter intensity $\lambda_c \bar{c}(\cdot)$ is given as 2.5×10^{-5}. The initial models for ten targets are given in Table II and the death time here refers to the last time a target exists.

Besides, the expansion coefficient of the Beta distribution is given as $|k_\beta| = 1.05$. The birth process is Poisson with parameters $J_\gamma = 4$, $\omega_\gamma = 0.01$ and $\widehat{P}_\gamma = \text{diag}([50, 50, 50, 50]^2)$. For each $j \in \{1, 2, 3, 4\}$, $\widehat{m}_{\gamma,1}^k = [-1500, 250, 0, 0]^\top$, $\widehat{m}_{\gamma,2}^k = [-250, 1000, 0, 0]^\top$, $\widehat{m}_{\gamma,3}^k = [250, 750, 0, 0]^\top$, $\widehat{m}_{\gamma,4}^k =$

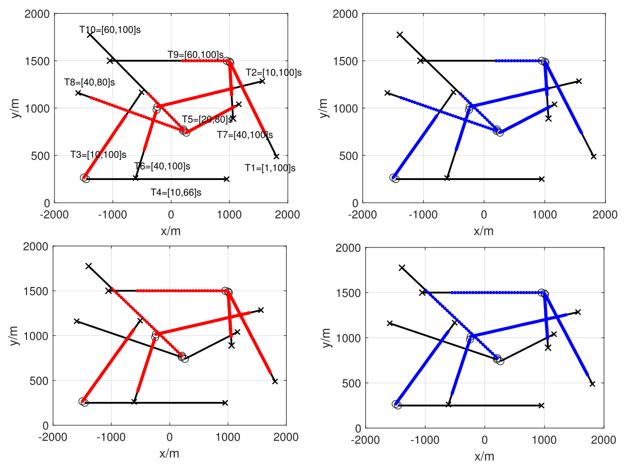

Fig. 1. The trajectory of BG-U-TCPHD (left) at 75 s (top), at 90 s (bottom), and the trajectory of BG-U-TPHD (right) at 75 s (top), at 90 s (bottom) with Beta distribution factors $u = 8, v = 2$.

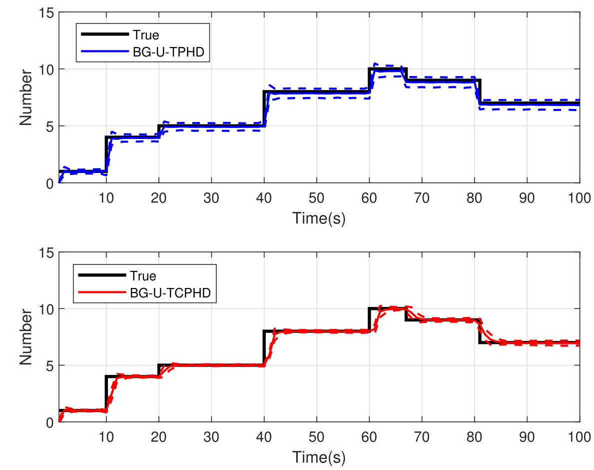

Fig. 2. The BG-U-TPHD filter (top) and the BG-U-TCPHD filter (bottom) with Beta distribution factors $u = 8, v = 2$, the solid lines represent the number estimation, and the dashed lines represent estimation after calculating the standard deviation.

$[1000, 1500, 0, 0]^\top$. In general cases, we are more interested in targets with detection probabilities greater than 0.5. Therefore, the Beta distribution factors of new born trajectories are given as $u = 8$ and $v = 2$, which means the initial value of detection probability is set as 0.8. Besides, the value of the L-scan approximation is set as $L = 5$.

The weight threshold of pruning is given as $\Gamma_p = 10^{-5}$, the threshold of absorption is given as $\Gamma_a = 4$ and the maximum of components is limited to $J_{\max} = 100$. For the BG-U-TCPHD filter, the cardinality distribution is capped at $N_{\max} = 100$.

By running 1500 Monte Carlo realizations, the performance of the BG-U-TPHD and BG-U-TCPHD filters are obtained as follows. To do so, the error $d^2(\mathbf{X}_k^s, \mathbf{X}_k)$ at time k between the estimated set of alive trajectories $\mathbf{X}_k^s$ and the truth $\mathbf{X}_k$ are measured by the metric for sets of trajectories, which is known as the trajectory metric (TM) error [46]. It is also considered to normalize the error by the corresponding time window k, thus, the root mean square (RMS) TM error $d(k)$ at the time k is obtained by

$$d(k) = \sqrt{\frac{1}{N_{mc}} \sum_{i=1}^{N_{mc}} d^2(\mathbf{X}_{k,i}^s, \mathbf{X}_k)/k}, \tag{106}$$

where $\mathbf{X}_{k,i}^s$ denotes the estimated set of alive trajectories at time k in the $i-th$ Monte Carlo run. The TM error also includes the error for the localization of detected targets, false targets, missed targets and track switches. In this paper, the parameters for the RMS TM error are set as $p = 2, c = 10, \gamma = 1$.

In Fig. 3, the GM-TPHD and GM-TCPHD filters [32] are based on assumptions of known detection profile. In other words, their tracking performance can be viewed as the performance upper bound of the BG-U-TPHD and BG-U-TCPHD filters, respectively. It can be seen from Figs. 1–3 that, both the BG-U-TPHD and BG-U-TCPHD filters can obtain excellent trajectory estimation which is close to that of the GM-TPHD and GM-TCPHD filters with the known detection profile [32]. In addition, the BG-U-TCPHD filter performs much better than

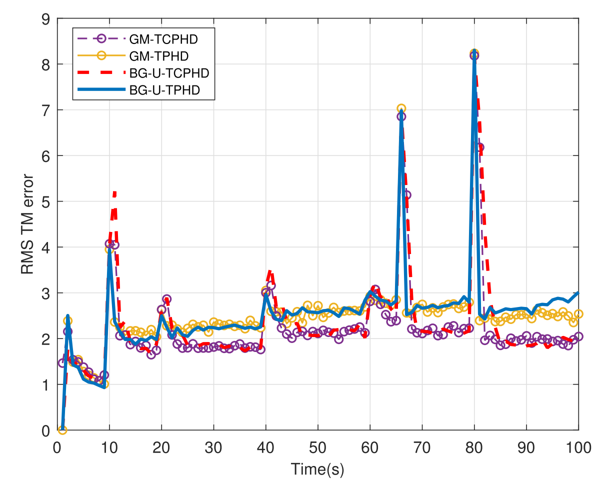

Fig. 3. The RMS trajectory metric error for the BG-U-TPHD and BG-U-TCPHD filters with $u = 8, v = 2$, as well as the GM-TPHD and GM-TCPHD filters with known detection probability.

the BG-U-TPHD filter, because the BG-U-TCPHD filter also propagates the cardinality distribution but the BG-U-TPHD filter does not. The decomposition of the RMS trajectory metric error for proposed filters is shown in Fig. 4. It shows that both filters possess a similar error for the localization and false targets, and they nearly have no track switch error. However, the error for missed targets in the BG-U-TCPHD filters is much lower than that in the BG-U-TPHD filter.

The value of the L-scan approximation is of great importance in both filters, so the influence of different values of the L-scan will be compared in detail. It can be seen from Fig. 5 that, with different values of the L-scan approximation, the BG-U-TCPHD filter always performs better than the BG-U-TPHD filter. Besides, it should be noted that, for both filters, the RMS TM error decreases when L increases, while the reduced amount gradually becomes less and less with increasing L. When L is bigger than

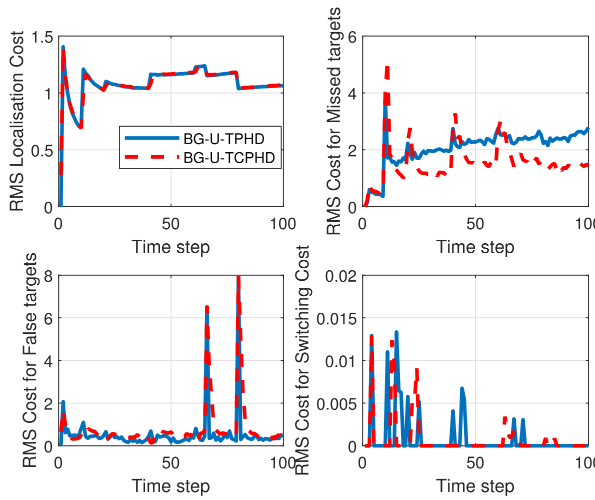

Fig. 4. The decomposition of the RMS trajectory metric error for the BG-U-TPHD and BG-U-TCPHD filters with $u = 8, v = 2$, including the error for the localization of detected targets, false targets, missed targets and track switches.

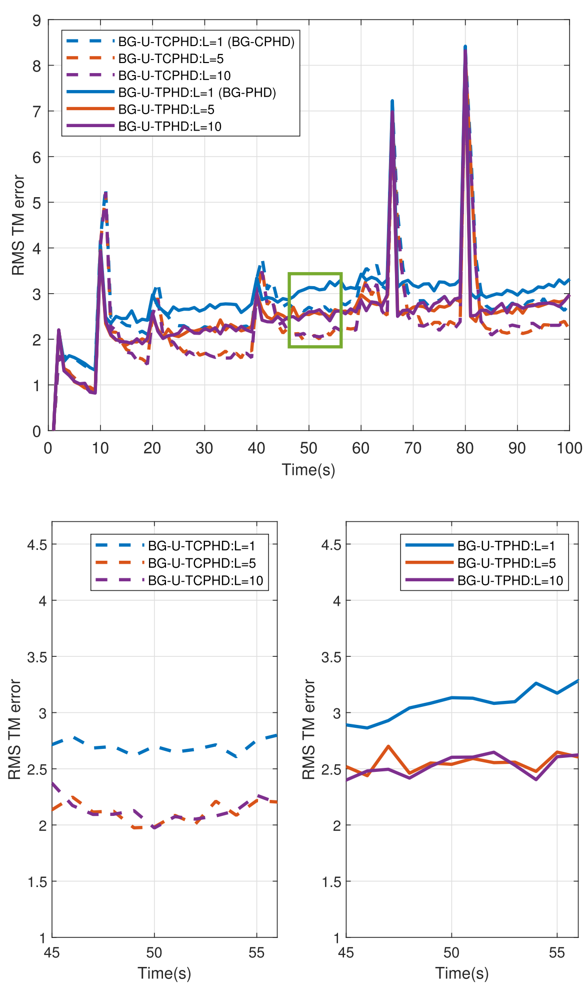

Fig. 5. The RMS TM error for the BG-U-TPHD and BG-U-TPHD filters with Beta distribution factors $u = 8, v = 2$ under the models of $L = 1, 5, 10$. The partial enlarged figure of the BG-U-TCPHD filter is shown in the bottom left and that of the BG-U-TPHD filter is shown in the bottom right.

TABLE III
THE RUN TIME(s) OF THE BG-U-TPHD AND BG-U-TPHD FILTERS

L	1	2	5	10	15	30	60
BG-U-TPHD	3.56	3.60	3.75	4.75	7.81	14.9	66.8
BG-U-TCPHD	4.12	4.13	4.25	5.15	8.12	15.5	68.1

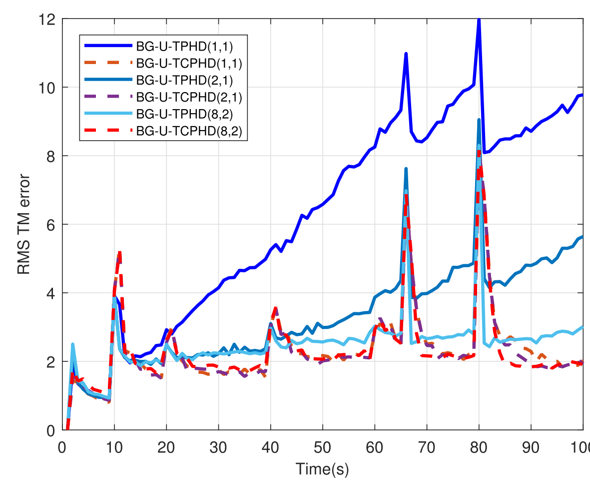

Fig. 6. The RMS trajectory metric error for the BG-U-TPHD and BG-U-TPHD filters with different Beta distribution factors ($L = 5$).

5, the performance nearly has no improvement. Meanwhile, the computational burden due to the increasing value of the L-scan approximation should also be concerned. The averaged time to run one Monte Carlo iteration with a 2.8 GHz Intel i7 laptop is listed in Table III.

From Table III, when L is less than 5, its decrease cannot effectively improve the calculation speed, while the computational cost sharply increases if L is bigger than 10. Considering both computational burden and estimation accuracy, L is usually a much smaller quantity than the length of the trajectory. Therefore, in the Scenario 1, the $L = 5$ is a suitable choice for both filters.

B. Scenario 2

In this section, we will focus on the performance of the BG-U-TPHD and BG-U-TCPHD filters with different Beta distribution factors, lower detection probability and uneven detection profile. First, the influence of different Beta distribution factors is elaborated and the uniform detection profile is adopted as $p_D = 0.98$ being the same as the Scenario 1. When the parameters of Beta distribution satisfy $u = 1, v = 1$, the Beta distribution equals to the uniform distribution. It can been seen from Fig. 6 that, both filters can respond faster to the change of cardinality and produce a smaller error when the initialization for detection probability is closer to the truth, while the BG-U-TPHD filter performs divergence when the initialization is far from the truth. In contrast, the BG-U-TCPHD filter is more robust.

Note that, compared to the robust BG-CPHD and BG-PHD filters in [38], the initialization of the Beta distribution factors is more important for the BG-U-TPHD and BG-U-TCPHD

TABLE IV
AVERAGE TM ERRORS FOR THE BG-U-TPHD AND BG-U-TCPHD FILTERS WITH DIFFERENT DETECTION PROBABILITIES

	BG-U-TPHD			BG-U-TCPHD		
(u,v)	(1,1)	(2,1)	(8,2)	(1,1)	(2,1)	(8,2)
$p_D = 0.98$	6.41	3.23	2.45	2.20	2.15	2.08
$p_D = 0.85$	11.51	9.80	6.15	4.24	4.04	3.80
$p_D = 0.73$	16.53	13.17	13.13	5.20	5.06	5.04

TABLE V
THE INITIAL TARGET STATES

	State	Birth Time/s	Death Time/s
Target 1	$[1005, 1489, 8, -10]^\top$	1	100
Target 2	$[-256, 1011, 20, 3]^\top$	20	80
Target 3	$[-1507, 257, 11, 10]^\top$	30	100

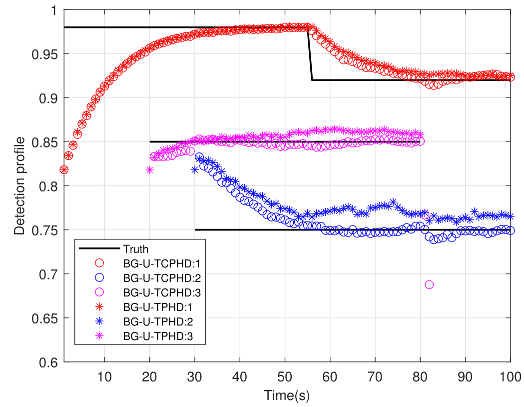

Fig. 7. The average estimation of the uneven detection profile for the BG-U-TPHD and BG-U-TCPHD filters. The detection probabilities of different targets are distinguished with different colors. Note that, the purple circles over 80 s are caused by the hysteresis of the BG-U-TCPHD filter for dead trajectories.

filters, especially for the former. Because the trajectory state of Beta-Gaussian component with the smaller weight is directly abandoned, as indicated by Table I. The trajectory estimation accuracy will decrease in the case of inaccurate estimation of detection probability. However, the merging procedure in the robust BG-CPHD and BG-PHD filters [38] can reduce this influence to some extent.

For targets with lower detection probabilities, from Table IV, the decrease of detection probability seriously worsens the performance of the BG-U-TPHD filter, but has a smaller effect on the BG-U-TCPHD filter.

For the case with uneven detection profile, we simplify Scenario 1 to three targets with different detection probabilities, which are given by the following equation

$$p_{D,j,k} = \begin{cases} 0.98, & j=1, k \leq 55 \\ 0.92, & j=1, k > 55 \\ 0.85, & j=2 \\ 0.75, & j=3 \end{cases} \tag{107}$$

where $j \in \{1,2,3\}$ denotes different targets and k denotes the time. The initial target states are listed in Table V and rest parameters are the same as Scenario 1. It can be seen from Fig. 7 that there is an initial settling in period, but after this miss distance, the estimation of detection profile converges to the truth and performs fluctuation with the changes of the number of targets. It turns out that the proposed BG-U-TPHD and BG-U-TCPHD filters provide the satisfactory performance of adaptively learning uneven detection profile, while the BG-U-TCPHD filter performs better.

VI. CONCLUSION

In this paper, we have derived the recursions of the U-TPHD and U-TCPHD filters by using the KLD minimization. Both filters can perform robustly in scenarios with unknown and time-varying target detection probability. Meanwhile, for the computation efficiency, the analytic recursions are also presented for the U-TPHD and U-TCPHD filters, which consider the effect of the unknown detection probability only at the latest frame time. The Beta-Gaussian mixture method is also adopted for the implementation of the proposed filters, which are referred to as the BG-U-TPHD and BG-U-TCPHD filters. Besides, the L-scan approximations of these filters are also presented. Finally, simulation results demonstrate that the BG-U-TPHD and BG-U-TCPHD filters can achieve robust tracking performance to adapt to unknown detection profile. Besides, it also shows that usually a small value of L in the L-scan approximation has similar performance than with a large value at a fraction of the computational cost.

APPENDIX A
PROOF OF PREDICTION

This section aims to clarify the relationship between the transition density of the augmented trajectory $\tilde{X} = (t, x^{1:i}, a^{1:i})$ and the transition density of augmented target (x, a). Taking the U-TPHD filter for example, the augmented trajectory state at time $k-1$ is given as $\underline{\tilde{X}} = (\underline{t}, \underline{x}^{1:\underline{i}}, \underline{a}^{1:\underline{i}})$ and the predicted augmented trajectory state at time k is given as $\tilde{X} = (t, x^{1:i}, a^{1:i})$. Thus, the prediction of the U-TPHD filter is obtained by

$$\begin{aligned} & D_{k|k-1}\left(\tilde{X}\right) \\ & = \gamma\left(\tilde{X}\right)\delta_1[i]\delta_k[t] + \int p_{S,k}\left(\underline{\tilde{X}}\right)\tilde{f}\left(\tilde{X}|\underline{\tilde{X}}\right)D_{k-1}\left(\underline{\tilde{X}}\right)d\underline{\tilde{X}}. \end{aligned} \tag{108}$$

We consider the transition function as the first-order Markov process and alive trajectories in the prediction step, so the above equation changes into:

$$\begin{aligned} & D_{k|k-1}\left(\tilde{X}\right) \\ & = \gamma\left(t, x^{1:i}, a^{1:i}\right)\delta_1[i]\delta_k[t] + p_{S,k}\left(x^{i-1}\right) f\left(x^i, a^i | x^{i-1}, a^{i-1}\right) \\ & \quad \times \iint \delta_{\underline{x}^{1:\underline{i}}}(x^{1:i-1})\delta_{\underline{a}^{1:\underline{i}}}(a^{1:i-1})\delta_{\underline{t}}[t]\delta_{\underline{i}+1}[i] \\ & \quad \times D_{k-1}\left(\underline{t}, \underline{x}^{1:\underline{i}}, \underline{a}^{1:\underline{i}}\right) d\underline{x}^{1:\underline{i}} d\underline{a}^{1:\underline{i}} \\ & = \gamma_k\left(\tilde{X}\right) + p_{S,k}\left(x^{i-1}\right) f\left(x^i, a^i | x^{i-1}, a^{i-1}\right) \end{aligned}$$

$$\times D_{k-1}\left(t, x^{1:i-1}, a^{1:i-1}\right), \tag{109}$$

where $\tilde{f}(\tilde{X}|\underline{\tilde{X}})$ and $f(x^i, a^i|x^{i-1}, a^{i-1})$ respectively denote the transition density of augmented trajectory and that of augmented target. As indicated by the (31), we consider the switch of detection probability is independent of the trajectory state, so the predicted PHD $D_{k|k-1}(\tilde{X})$ can be simplified as follows, which is the same as (34):

$$D_{k|k-1}(\tilde{X}) = \gamma_k(\tilde{X}) + p_{S,k}\left(x^{i-1}\right) f\left(x^i|x^{i-1}, a^{i-1}\right) \\ \times g\left(a^i|a^{i-1}\right) D_{k-1}\left(t, x^{1:i-1}, a^{1:i-1}\right),$$

where $g(\cdot|\cdot)$ denotes the transition density of detection probability. The prediction of the U-TCPHD filter uses the same principle but also considers the cardinality distribution, which is a simple extension of [32]. So it is omitted here.

Appendix B
Proof of Proposition 2

In this appendix, the proof of Proposition 2 is elaborated. The proof of KLD minimization is omitted, because the trajectory augmented with a detection probability sequence is a simple extension of the classical trajectory state, and the proof of the latter can be found in [32]. First, Given a set of augmented targets $\{\tilde{x}_1, \ldots, \tilde{x}_n\}$, the density of measurements Z_k at time k is given as

$$\begin{aligned} &\ell_k^\tau(Z_k|\{\tilde{x}_1, \ldots, \tilde{x}_n\}) \\ &= e^{-\lambda_c}\left[\prod_{j=1} \lambda_c \bar{c}(z_j)\right]\left[\prod_{j=1}^{n}(1-a_j)\right] \\ &\quad \times \sum_{\sigma\in\Gamma_n} \prod_{j:\sigma_j>0} \frac{a_j \cdot l_k(z_{\sigma_j}|x_j)}{(1-a_j)\lambda_c \bar{c}(z_{\sigma_j})}, \end{aligned} \tag{110}$$

where Γ_n denotes all kinds of possible associations between n targets and a set of measurements σ. The notation $\sigma_j > 0$ indicates the target j is detected and associated with measurements σ_j. Here, the notation a denotes a^{k-t+1}, which represents the detection profile at time k. Given a set of augmented trajectories $\tilde{\mathbf{X}}_k = \{\tilde{X}_1, \ldots, \tilde{X}_n\}$ at time k, the posterior PHD of the augmented multi-trajectory density can be obtained by Bayes rule

$$\begin{aligned} &D_k(\tilde{X}) \\ &= \frac{1}{\ell_k(Z_k)} \int \ell_k\left(Z_k|\{\tilde{X}\}\cup\tilde{\mathbf{X}}_k\right) p_{k|k-1}\left(\{\tilde{X}\}\cup\tilde{\mathbf{X}}_k\right)\delta\tilde{\mathbf{X}}_k \\ &= \frac{1}{\ell_k(Z_k)} \sum_{n=0}^{\infty} \frac{1}{n!} \int \ell_k\left(Z_k|\{\tilde{X}, \tilde{X}_1, \ldots, \tilde{X}_n\}\right) \\ &\quad \times p_{k|k-1}\left(\{\tilde{X}, \tilde{X}_1, \ldots, \tilde{X}_n\}\right)\delta\tilde{X}_{1:n} \\ &= \frac{D_{k|k-1}(\tilde{X})}{\ell_k(Z_k)} \sum_{n=0}^{\infty} \frac{1}{n!} \int \ell_k^\tau\left(Z_k|\{\tilde{x}, \tilde{x}_1, \ldots, \tilde{x}_n\}\right) \\ &\quad \times e^{-\lambda} \prod_{j=1}^{n} D_{k|k-1}^\tau(\tilde{x}_j)\delta\tilde{x}_{1:n}, \end{aligned} \tag{111}$$

where

$$D_k^\tau(x, a) = \sum_{t=1}^{k} \iint D_k(t, x^{1:k-t}, a^{1:k-t}, x, a)da^{1:k-t}dx^{1:k-t},$$

which is the PHD of the posterior density of augmented targets at time k. It integrates the information about the sequence of both detection probabilities and past target states. The measurement set Z_k comes from the clutter and targets. Therefore the denominator of the Bayes rule is obtained as

$$\ell_k(Z_k) = e^{-\lambda_c - \iint a\cdot D_{k|k-1}^\tau(x,a)dadx} \\ \times \prod_{z\in Z_k}\left[\lambda_c\bar{c}(z) + \iint a\cdot l(z|x)D_{k|k-1}^\tau(x,a)dadx\right]. \tag{112}$$

Based on [21], at time k, the target x can be detected, with probability a (depending on its corresponding augmented part) or miss detection with probability $1-a$. Therefore, we can obtain

$$\begin{aligned} &\ell_k^\tau(Z_k|\{\tilde{x}, \tilde{x}_1, \ldots, \tilde{x}_n\}) \\ &= (1-a)\cdot\ell_k^\tau(Z_k|\{\tilde{x}_1, \ldots, \tilde{x}_n\}) \\ &\quad + a\sum_{z\in Z_k} l_k(z|x)\ell_k^\tau(Z_k\backslash\{z\}|\{\tilde{x}_1, \ldots, \tilde{x}_n\}). \end{aligned} \tag{113}$$

The posterior PHD of the augmented multi-trajectory density is

$$\begin{aligned} D_k\left(\tilde{X}\right) &= D_{k|k-1}\left(\tilde{X}\right)(1-a) \\ &\quad + D_{k|k-1}\left(\tilde{X}\right)a \\ &\quad \times \sum_{z\in Z_k} \frac{l_k(z|x)}{\lambda_c\bar{c}(z) + \iint a\cdot l_k(z|x)D_{k|k-1}^\tau(x,a)dadx}. \end{aligned} \tag{114}$$

Appendix C
Proof of Proposition 4

In this appendix, the proof of Proposition 4 is described in detail. Similar to Appendix A, the posterior PHD can be obtained by the Bayes rule

$$\begin{aligned} &D_k(\tilde{X}) \\ &= \frac{1}{\ell_k(Z_k)} \sum_{n=0}^{\infty} \frac{1}{n!} \int \ell_k\left(Z_k|\{\tilde{X}, \tilde{X}_1, \ldots, \tilde{X}_n\}\right) \\ &\quad \times p_{k|k-1}\left(\{\tilde{X}, \tilde{X}_1, \ldots, \tilde{X}_n\}\right)\delta\tilde{X}_{1:n} \\ &= \frac{1}{\ell_k(Z_k)} \sum_{n=0}^{\infty}(n+1) \int \ell_k\left(Z_k|\{\tilde{X}, \tilde{X}_1, \ldots, \tilde{X}_n\}\right) \end{aligned}$$

$$\times \rho_{k|k-1}(n+1)\bar{p}_{k|k-1}(\tilde{X})\prod_{j=1}^{n}\bar{p}_{k|k-1}(\tilde{X}_j)\delta\tilde{X}_{1:n}. \quad (115)$$

where

$$\int \ell_k\left(Z_k|\{\tilde{X}_1,\ldots,\tilde{X}_n\}\right)\prod_{i=1}^{n}\bar{p}_{k|k-1}(\tilde{X}_i)\delta\tilde{X}_{1:n}$$
$$= \prod_{j=1}^{|Z_k|=M}\bar{c}(z_j)\sum_{i=0}^{\min(M,n)}(M-i)!\rho_{c,k}(M-i)\frac{n!}{(n-i)!}$$
$$\times\frac{\left[\iint(1-a)D^{\tau}_{k|k-1}(x,a)dadx\right]^{n-i}}{\left[\iint D^{\tau}_{k|k-1}(x,a)dadx\right]^{n}}$$
$$\times\sum_{S_k\subseteq Z_k,|S_k|=i}\frac{\prod_{j=1}^{i}\left[\iint a\cdot l(z_j|x)D^{\tau}_{k|k-1}(x,a))dadx\right]}{\prod_{j=1}^{i}\bar{c}(z_j)}$$
$$= \prod_{z\in Z_k}\bar{c}(z)\Upsilon^0_k\left[D^{\tau}_{k|k-1};Z_k\right](n). \quad (116)$$

Based on the theory of [21], we can obtain

$$\sum_{n=0}^{\infty}(n+1)\rho_{k|k-1}(n+1)\int\ell_k\left(Z_k|\{\tilde{X}_1,\ldots,\tilde{X}_n\}\right)$$
$$\times\prod_{i=1}^{n}\bar{p}_{k|k-1}(\tilde{X}_i)\delta\tilde{X}_{1:n}$$
$$= \iint D^{\tau}_{k|k-1}(x,a)dxda\langle\rho_{k|k-1},\Upsilon^1_k[D^{\tau}_{k|k-1};Z_k]\rangle\prod_{z\in Z_k}\bar{c}(z). \quad (117)$$

The denominator of Bayes rule is

$$\ell_k\left(Z_k\right) = \prod_{z\in Z_k}\bar{c}(z)\langle\rho_{k|k-1},\Upsilon^0_k[D^{\tau}_{k|k-1};Z_k]\rangle. \quad (118)$$

Therefore, the posterior PHD of the augmented multi-trajectory density is given as

$$D_k\left(\tilde{X}\right) = D_{k|k-1}\left(\tilde{X}\right)(1-a)$$
$$\times\frac{\left\langle\Upsilon^1_k\left[D^{\tau}_{k|k-1};Z_k\right],\rho_{k|k-1}\right\rangle}{\left\langle\Upsilon^0_k\left[D^{\tau}_{k|k-1};Z_k\right],\rho_{k|k-1}\right\rangle}$$
$$+ D_{k|k-1}\left(\tilde{X}\right)a$$
$$\times\sum_{z\in Z_k}\frac{l_k(z|x)}{\bar{c}(z)}\frac{\left\langle\Upsilon^1_k\left[D^{\tau}_{k|k-1};Z_k\backslash\{z\}\right],\rho_{k|k-1}\right\rangle}{\left\langle\Upsilon^0_k\left[D^{\tau}_{k|k-1};Z_k\right],\rho_{k|k-1}\right\rangle}. \quad (119)$$

Besides, the posterior cardinality distribution is also given by Bayesian recursion

$$\rho_k(n) = \frac{1}{\ell(Z_k)n!}\int\ell(Z_k|\{\tilde{X}_1,\ldots,\tilde{X}_n\})$$
$$\times p_{k|k-1}(\{\tilde{X}_1,\ldots,\tilde{X}_n\})\delta\tilde{X}_{1:n}$$
$$= \frac{\Upsilon^0_k\left[D^{\tau}_{k|k-1};Z_k\right](n)\rho_{k|k-1}(n)}{\left\langle\Upsilon^0_k\left[D^{\tau}_{k|k-1};Z_k\right],\rho_{k|k-1}\right\rangle}. \quad (120)$$

REFERENCES

[1] S. Blackman, *Multiple Target Tracking With Radar Applications*. Norwood, MA: Artech House, 1986.

[2] K. Dai, Y. Wang, H. D. Q. Ji, and C. Yin, “Multiple vehicle tracking based on labeled multiple Bernoulli filter using pre-clustered laser range finder data,” *IEEE Trans. Veh. Technol.*, vol. 68, no. 11, pp. 10382–10393, Nov. 2019.

[3] V. Savic, H. Wymeersch, and E. G. Larsson, “Target tracking in confined environments with uncertain sensor positions,” *IEEE Trans. Veh. Technol.*, vol. 65, no. 2, pp. 870–882, Feb. 2016.

[4] W. Yi, Z. Fang, W. Li, R. Hoseinnezhad, and L. Kong, “Multi-frame track-before-detect algorithm for maneuvering target tracking,” *IEEE Trans. Veh. Technol.*, vol. 69, no. 4, pp. 4104–4118, Apr. 2020.

[5] W. Yeow, C. Tham, and W. Wong, “Energy efficient multiple target tracking in wireless sensor networks,” *IEEE Trans. Veh. Technol.*, vol. 56, no. 2, pp. 918–928, Mar. 2007.

[6] W. Yi, Y. Yuan, R. Hoseinnezhad, and L. Kong, “Resource scheduling for distributed multi-target tracking in netted colocated MIMO radar systems,” *IEEE Trans. Signal Process.*, vol. 68, pp. 1602–1617, 2021.

[7] Y. Bar-Shalom and T. E. Fortmann, *Tracking and Data Association*. San Francisco, CA, USA: Academic, 1998.

[8] T. E. Fortmann, Y. Bar-Shalom, and M. Scheffe, “Sonar tracking of multiple targets using joint probabilistic data association,” *IEEE J. Ocean. Eng.*, vol. 8, no. 3, pp. 173–184, Jul. 1983.

[9] S. Blackman, “Multiple hypothesis tracking for multiple target tracking,” *IEEE Aerosp. Electron. Syst. Mag.*, vol. 19, no. 1, pp. 5–18, Jan. 2004.

[10] R. Mahler, *Statistical Multisource Multitarget Information Fusion*. Norwood, MA, USA: Artech House, 2007.

[11] R. Mahler, “Multi-target Bayes filter via first-order multi-target moments,” *IEEE Trans. Aerosp. Electron. Syst.*, vol. 39, no. 4, pp. 1152–1178, Oct. 2003.

[12] B.-N. Vo and W.-K. Ma, “The Gaussian mixture probability hypothesis density filter,” *IEEE Trans. Signal Process.*, vol. 54, no. 11, pp. 4091–4104, Nov. 2006.

[13] R. Mahler, “PHD filters of higher order in target number,” *IEEE Trans. Aerosp. Electron. Syst.*, vol. 43, no. 4, pp. 1523–1543, Oct. 2007.

[14] B.-N. Vo and A. Cantoni, “Analytic implementations of the cardinalized probability hypothesis density filter,” *IEEE Trans. Signal Process.*, vol. 55, no. 7, pp. 3553–3567, Jul. 2007.

[15] B.-T. Vo, B.-N. Vo, and A. Cantoni, “The cardinality balanced multi-target multi-Bernoulli filter and its implementations,” *IEEE Trans. Signal Process.*, vol. 57, no. 2, pp. 409–423, Feb. 2009.

[16] J. L. Williams, “Marginal multi-Bernoulli filters: RFS derivation of MHT, JIPDA and association-based member,” *IEEE Trans. Aerosp. Electron. Syst.*, vol. 51, no. 3, pp. 1664–1687, Jul. 2015.

[17] A. F. García-Fernández, J. L. Williams, K. Granström, and L. Svensson, “Poisson multi-Bernoulli mixture filter: Direct derivation and implementation,” *IEEE Trans. Aerosp. Electron. Syst.*, vol. 54, no. 4, pp. 1883–1901, Aug. 2018.

[18] B.-T. Vo and B.-N. Vo, “Labeled random finite sets and multi-object conjugate priors,” *IEEE Trans. Signal Process.*, vol. 61, no. 13, pp. 3460–3475, Jul. 2013.

[19] B.-T. Vo, B.-N. Vo, and D. Phung, “Labeled random finite sets and the Bayes multi-target tracking filter,” *IEEE Trans. Signal Process.*, vol. 62, no. 24, pp. 6554–6567, Dec. 2014.

[20] S. Reuter, B.-T. Vo, B.-N. Vo, and K. Dietmayer, “The labeled multi-Bernoulli filter,” *IEEE Trans. Signal Process.*, vol. 62, no. 12, pp. 3246–3260, Jun. 2014.

[21] A. F. García-Fernández and B.-N. Vo, “Derivation of the PHD and CPHD filters based on direct Kullback-Leibler divergence minimization,” *IEEE Trans. Signal Process.*, vol. 63, no. 21, pp. 5812–5820, Nov. 2015.

[22] B.-N. Vo, S. Singh, and A. Doucet, “Sequential Monte Carlo methods for multi-target filtering with random finite sets,” *IEEE Trans. Aerosp. Electron. Syst.*, vol. 41, no. 4, pp. 1224–1245, Oct. 2005.

[23] B. Ristic, D. Clark, and B.-N. Vo, “Improved SMC implementation of the PHD filter,” in *Proc. Int. Conf. Inf. Fusion*, 2010, pp. 1–8.

[24] G. Battistelli, L. Chisci, C. Fantacci, A. Farina, and A. Graziano, “Consensus CPHD filter for distributed multitarget tracking,” *IEEE J. Sel. Topics Signal Process.*, vol. 7, no. 3, pp. 508–520, Jun. 2013.

[25] M. Uney, D. E. Clark, and S. J. Julier, “Distributed fusion of PHD filters via exponential mixture densities,” *IEEE J. Sel. Topics Signal Process.*, vol. 7, no. 3, pp. 521–531, Jun. 2013.

[26] L. Gao, G. Battistelli, and L. Chisci, “Random-finite-set-based distributed multirobot SLAM,” *IEEE J. Sel. Topics Signal Process.*, vol. 36, no. 6, pp. 1758–1777, Dec. 2020.

[27] J. Mullane, B.-N. Vo, M. D. Adams, and B.-T. Vo, “A random-finite-set approach to Bayesian SLAM,” *IEEE Trans. Robot.*, vol. 27, no. 2, pp. 268–282, Apr. 2011.

[28] E. Maggio, M. Taj, and A. Cavallaro, “Efficient multitarget visual tracking using random finite sets,” *IEEE Trans. Circuits Syst. Video Technol.*, vol. 18, no. 8, pp. 1016–1027, Aug. 2008.

[29] B. H. X. Zhou, Y. Li, and T. Bai, “GM-PHD-based multi-target visual tracking using entropy distribution and game theory,” *IEEE Trans. Ind. Informat.*, vol. 10, no. 2, pp. 1064–1076, May 2014.

[30] B.-N. Vo and B.-T. Vo, “A multi-scan labeled random finite set model for multi-object state estimation,” *IEEE Trans. Signal Process.*, vol. 67, no. 19, pp. 1003–1016, Oct. 2019.

[31] L. Svensson and M. Morelande, “Target tracking based on estimation of sets of trajectories,” in *Proc. 17th Int. Conf. Inf. Fusion*, 2014, pp. 1–8.

[32] A. F. García-Fernández and L. Svensson, “Trajectory PHD and CPHD filters,” *IEEE Trans. Signal Process.*, vol. 67, no. 22, pp. 1003–1016, Nov. 2019.

[33] A. F. García-Fernández, L. Svensson, J. L. Williams, Y. Xia, and K. Granström, “Trajectory multi-Bernoulli filters for multi-target tracking based on sets of trajectories,” in *Proc. 23rd Int. Conf. Inf. Fusion*, 2020, pp. 1003–1016.

[34] K. Granström, L. Svensson, Y. Xia, and J. L. Williams, “Poisson multi-Bernoulli mixture trackers: Continuity through random finite sets of trajectories,” in *Proc. 21st Int. Conf. Inf. Fusion*, 2018, pp. 973–981.

[35] R. Mahler, “CPHD and PHD filters for unknown backgrounds, II: Multitarget filtering in dynamic clutter,” in *Proc. SPIE*, vol. 7330, 2009.

[36] X. Chen, R. Tharmarasa, M. Pelletier, and T. Kirubarajan, “Integrated clutter estimation and target tracking using Poisson point processes,” *IEEE Trans. Aerosp. Electron. Syst.*, vol. 48, no. 2, pp. 1210–1235, Apr. 2012.

[37] R. Mahler and B.-T. Vo, “An improved CPHD filter for unknown clutter backgrounds,” in *Proc. SPIE*, vol. 9091, 2014.

[38] R. Mahler, B.-T. Vo, and B.-N. Vo, “CPHD filtering with unknown clutter rate and detection profile,” *IEEE Trans. Signal Process.*, vol. 59, no. 8, pp. 3497–3513, Aug. 2011.

[39] Y. G. Punchihewa, B.-T. Vo, B.-N. Vo, and D. Y. Kim, “Multisensor adaptive Bayesian tracking under time-varying target detection probability,” *IEEE Trans. Aerosp. Electron. Syst.*, vol. 52, no. 5, pp. 2193–2209, Oct. 2016.

[40] G. Li, L. Kong, W. Yi, and X. Li, “Robust Poisson multi-Bernoulli mixture filter with unknown detection probability,” *IEEE Trans. Veh. Technol.*, vol. 70, no. 1, pp. 886–899, Jan. 2020.

[41] Y. G. Punchihewa, B.-T. Vo, B.-N. Vo, and D. Y. Kim, “Multiple object tracking in unknown backgrounds with labeled random finite sets,” *IEEE Trans. Signal Process.*, vol. 66, no. 11, pp. 3040–3055, Jun. 2018.

[42] B.-T. Vo, B.-N. Vo, R. Hoseinnezhad, and R. Mahler, “Robust multi-Bernoulli filtering,” *IEEE J. Sel. Topics Signal Process.*, vol. 7, no. 3, pp. 399–409, Jun. 2013.

[43] C. Li, W. Wang, T. Kirubarajan, J. Sun, and P. Lei, “PHD and CPHD filtering with unknown detection probability,” *IEEE Trans. Signal Process.*, vol. 66, no. 14, pp. 3784–3798, Jul. 2018.

[44] A. F. García-Fernández, L. Svensson, and M. R. Morelande, “Multiple target tracking based on sets of trajectories,” *IEEE Trans. Aerosp. Electron. Syst.*, vol. 56, no. 3, pp. 1685–1707, Jun. 2020.

[45] P. Borwein and T. Erdlyi, *Newton’s Identities Section 1.1.E.2 in Polynomials and Polynomial Inequalities*. Berlin, Germany: Springer, 1995.

[46] A. F. García-Fernández, A. S. Rahmathullah, and L. Svensson, “A metric on the space of finite sets of trajectories for evaluation of multi-target tracking algorithms,” *IEEE Trans. Signal Process.*, vol. 68, pp. 3917–3928, 2020.

Shaoxiu Wei is currently working toward the B.E. degree in communication engineering with the University of Electronic Science and Technology of China, Chengdu, China. His research interests include statistical signal processing and multitarget tracking.

Boxiang Zhang received the B.S. degree from the School of Information and Communication Engineering, University of Electronic Science and Technology of China, Chengdu, China, where he is currently working toward the Ph.D. degree in signal and information processing. His research interests include RFS method based multitarget tracking and maneuvering target tracking.

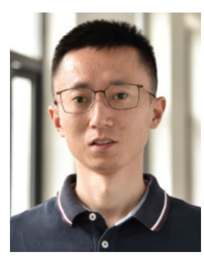

Wei Yi (Senior Member, IEEE) received the B.E. and the Ph.D. degrees in electronic engineering from the University of Electronic Science and Technology of China (UESTC), Chengdu, China, in 2006 and 2012, respectively. From 2010 to 2012, he was a Visiting Student with the Melbourne Systems Laboratory, University of Melbourne, Melbourne, VIC, Australia. From 2013 to 2015, he was a Senior Lecturer, and was promoted as an Associate Professor in 2015, with the School of Information and Communication Engineering, UESTC. He was the recipient of the Best Student Paper Competition–First place winner at the 2012 IEEE Radar Conference, Atlanta, Best Student Paper Award at the 15th International Conference on Information Fusion, Singapore, 2012, and also co-recipient of the Best Student Paper Award at the 21st International Conference on Information Fusion, Cambridge, 2018. He served on the editorial boards of the *Journal of Radars*, and is the Guest Editor of MDPI *Sensors*. He was a regular corresponding expert of *Frontiers of Information Technology & Electronic Engineering*. He was also the Organizing Co-Chair, General Co-Chair and Publication Co-Chair of *ICCAIS* in 2018, 2019, and 2020, respectively.